NASA CR-177857

Final Project Report

NASA Contract NAS5-28617

"Constraints on Geomagnetic Secular Variation Modeling from Electromagnetism and Fluid Dynamics of the Earth's Core"

Covering work performed between
18 October 1984 and 28 February 1986

Principal Investigator:

Prof. Edward R. Benton
Campus Box 391
Dept. of Astrophysical, Planetary & Atmospheric Sciences
University of Colorado
Boulder, CO 80309
Telephone. (303) 492-7988

28 February 1986

(NASA-CR-177857) CONSTRAINTS ON GEOMAGNETIC SECULAR VARIATION MODELING FROM ELECTROMAGNETISM AND FLUID DYNAMICS OF THE EARTH'S CORE Final Report, 18 Oct. 1984 - 28 Feb. 1986 (Colcrado Univ.) 58 p G3/46

N86-24063

Unclas 09117

Introduction

The work performed under this three year project is the result of a collaborative, but separately funded, effort between Edward R. Benton of the University of Colorado, Ronald H. Estes of Science Applications Research, Inc. (formerly of Businesss and Technological Systems, Inc.) and Robert A. Langel of the NASA Goddard Space Flight Center. Theoretical work of Professor Benton has been funded under NASA Contracts NAS5-27671 (covering the period from 18 May 1983 through 17 October 1984) and NAS5-28617 (for the period from 9 November 1984 through 28 February 1986) to the University of Colorado. Development of geomagnetic field models and appropriate algorithms by Mr. Estes is funded under NASA Contract NAS5-28671 to Business and Technological Systems, Inc. Dr. Langel serves as co-investigator to this joint project.

During the contract period now ending, work at the University of Colorado has concentrated first on preparing a paper that describes and derives a set of physical constraints for geomagnetic field modeling that form the theoretical basis for this project. That work, now published, is attached as a part of this report. The work initiated this past year is the detailed implementation of that theory in a new set of geomagnetic field models so constructed that they satisfy (approximately) a subset of the constraints derived in the above paper. This latter work was presented (orally) at the Vth Scientific Assembly of IAGA

(International Association of Geomagetism and Aeronomy), Prague, Czechoslovakia, August 1985. It has been written up for publication in Physics of the Earth and Planetary Interiors under the co-authorship of Benton, Estes and Langel. It gives a full, accurate, yet concise descripton of our joint activities and progress during the past year, so it is included as the main part of this report. The major conclusions reached are that the incorporation into geomagnetic field models of non-linear constraints that arise from consideration of the physics and dynamics of the earth's core, is numerically feasible and leads to better short range predictability than do unconstrained models

In the next time period we intend to extend the preliminary models constructed so far by lengthening the data interval and incorporating a greater number of constraints. We will also explore alternative representation to low order polynomials for the time dependence of secular variation.

Other pieces of work, that were partially supported by this project include:

Benton, E.R., and Alldredge, L.R., "On the Interpretation of the Geomagnetic Energy Spectrum," 44 page typescript submitted to Physics of the Earth and Planetary Interiors, October 1985.

Voorhies, C.V., "Steady Flows at the Top of Earth's Core Derived from Geomagnetic Field Models," 95 page typescript submitted to Journal of Geophysical Research, January 1986.

Voorhies, C.V. and Backus, G.E., "Steady Flows at the Top of the Core from Geomagnetic Field Models: The Steady Motions Theorem," Geophysical and Astrophysical Fluid Dynamics, **32**, 163-173, 1985.

Geomagnetic Field Modeling Incorporating Constraints from Frozen-Flux Electromagnetism

Edward R. Benton

Dept. of Astrophysical, Planetary & Atmospheric Sciences
Campus Box 391
University of Colorado
Boulder, CO 80309

Ronald H. Estes

Science Applications Research, Inc.
4400 Forbes Blvd
Lanham, MD 20706

Robert A. Langel

Code 622, Geophysics Branch
NASA/Goddard Space Flight Center
Greenbelt, MD 20771

Abstract

A spherical harmonic representation of the geomagnetic field and its secular variation for epoch 1980, designated GSFC(9/84), is derived and evaluated. At three epochs (1977.5, 1980.0, 1982.5) this model incorporates conservation of magnetic flux through five selected patches of area on the core-mantle boundary bounded by the zero contours of vertical magnetic field. These fifteen non-linear constraints are included like data in an iterative least squares parameter estimation procedure that starts with the recently derived unconstrained field model designated GSFC(12/83), Langel and Estes (1985). Convergence is approached within three iterations.

The constrained model is evaluated by comparing its predictive capability outside the time span of its data, in terms of residuals at magnetic observatories, with that for the unconstrained model. The new model demonstrates significantly improved predictability.

Next, it is established that the flux of magnetic secular variation out of the northern (or southern) geographic hemisphere of the core-mantle boundary is nearly conserved by a remake of the field model designated GSFC(9/80). The GSFC(9/84) model is then examined and found to satisfy this independent linear constraint on secular variation very well.

1. Introduction

Advances in geomagnetic field modeling typically involve a sequence of steps. First, a new theoretical concept is put forward. Then it is tested against data. Finally, if the tests are passed, the concept is adopted and incorporated into standard modeling procedure. An early example of this chain of events began with Gilbert's announced belief in 1600 that the Earth itself is the source of the observed magnetic field. This idea was confirmed in 1839 by Gauss, whose spherical harmonic analysis of existing data clearly showed that the part of the geomagnetic field originating from sources outside the Earth was insignificant compared to the main field of internal origin. As a result, it is now standard modeling practice to ignore external fields from the outset (actually, recent satellite data are sufficiently extensive that some modelers have again begun to restore the very low harmonics of the external field into their data fitting algorithms).

A modern version of this same process can be thought of as originating when Roberts and Scott (1965) advocated that a hydromagnetic hypothesis be invoked to assist in modeling short-term geomagnetic secular variation. Their idea was that, during short enough time intervals, there would be insufficient time for magnetic diffusion to separate fluid parcels in the earth's core from magnetic field lines. One important consequence of this "frozen-flux hypothesis" is that magnetic flux tubes bounded by curves just below the

core-mantle boundary (CMB) which always consist of the same fluid parcels then move laterally with the fluid and conserve their strength. Backus (1968) discovered that the contours on which the vertical magnetic field vanishes on the CMB, called "null-flux curves," constitute such moving fluid boundaries of material magnetic flux tubes. Then Hide (1978) pointed out the following way to test the frozen-flux concept against data from seismology. Roberts and Scott (1965) had noticed that even though the absolute magnetic flux crossing any geocentric spherical surface of radius $r > b$, where b is the radius of the CMB, can change in time; yet, the absolute flux crossing the top of a perfectly conducting core is invariant in time. Hide (1978) proposed to evaluate the absolute flux integral (or pole strength, after Bondi and Gold, 1950)

$$P(r,t) \equiv \int_0^{2\pi}\int_0^{\pi} |B_r(r,\theta,\phi,t)| \sin\theta d\theta d\phi, \qquad (1)$$

for various radii and times. Here B_r is the vertical magnetic field at time t in spherical coordinates r, θ, ϕ, with θ, co-latitude, ϕ, east longitude. With r decreasing from the Earth's surface, the value $r = b$ would be that radius at which P first becomes stationary in time.

Hide and Malin (1981) used the above magnetic method for determining the radius of the Earth's core and achieved moderate success. Voorhies and Benton (1982), adopting a different technique and more recent data, achieved agreement with the seismic value for b (3485 km) to within 1.8%. The average

of many further determinations by Voorhies (1984) agreees to within 0.6%, so there is good evidence for believing the global aspect of the frozen-flux hypothesis on short time scales.

A significant body of literature that either tests or uses the frozen-flux hypothesis now exists (a representative sample includes Backus and Le Mouel 1986; Benton 1979a,b, 1981a,b; Benton and Muth 1979; Bloxham and Gubbins 1985, 1986; Gubbins 1982, 1983, 1984; Gubbins and Bloxham, 1985; Gubbins and Roberts 1983, Le Mouel et al., 1984; Madden and LeMouel 1982; Shure et al., 1983; Voorhies and Backus, 1985; Voorhies and Benton 1982; Whaler 1980, 1982, 1984). The time therefore appears to be appropriate to begin incorporating into short-term field modeling at least global and probably regional constraints from the frozen-flux theory of the core. The qualifier "short-term" here is because the assumption of no flux diffusion must fail on sufficiently long time scales (as well as on too short length scales) Backus (1968), Booker (1969). Voorhies (1984), and Bloxham and Gubbins (1985) find evidence for possible flux diffusion in a small null-flux patch beneath the South Atlantic (unfortunately, an area not sampled by the network of magnetic observatories). As a result, we believe it vital to test thoroughly any field model constrained by frozen-flux. Bloxham and Gubbins (1985) recently introduced into a field model conservation of magnetic flux in each patch of area on the CMB bounded by a null-flux curve. They applied their method to

observatory data at 1959.5, observatory plus POGO data at 1969.5, and MAGSAT data at 1980. They tested the constrained model by comparing its estimated modeling errors with the misfit between the model and its data and concluded, tentatively , that flux was not conserved. Yet, as they note, this sort of test is very heavily colored by the reliability of their error estimates.

In this paper we employ a similar iterative penalty method (Luenberger, 1973) to a linearized form of only that subset of flux conservation integrals which are believed to involve well-determined null-flux curves so that the frozen-flux assumption is appropriate. Moreover, the time span of the data used is only the five years centered on 1980 to ensure that flux diffusion should be minimal. We also introduce two quite different tests of the constrained model which are independent of error estimates. In the first test both unconstrained and constrained models are constructed from the same starting data set. Then their ability to hindcast and to forecast the magnetic field before and after the time interval spanning the data input are compared by examining the temporal growth of model residuals to observatory data. The second test involves first invoking a new fluid dynamical assumption to simplify the vertical angular momentum balance at the top of the core (Benton, 1985). If the unsteady change in vertical absolute vorticity is produced entirely by Coriolis and inertial torques on a fluid parcel, then one predicts that the total (not absolute) magnetic flux out of either the northern or

southern geographic hemisphere of the CMB is conserved by a perfectly conducting core. Time differentiation then provides a simple linear, analytic constraint on the zonal secular variation coefficients of odd degree. Instead of invoking this "magnetic constraint from vorticity dynamics" into our field models we first test it by devloping a high quality field model (a remake of the GSFC(9/80) model) containing no frozen-flux constraints whatever. Finding that its zeroth order, odd degree secular variation coefficients do indeed satisfy the above linear constraint rather well, we then examine the field model GSFC(9/84) to determine whether or not it too obeys this constraint.

In Section 2, we describe the frozen-flux constraints of interest. Then, in Section 3 the mathematical technique for least squares minimization incorporating non-linear constraints like additional data is introduced. The new constrained model, GSFC(9/84), and its unconstrained counterpart are developed in Section 4 and assessed in Section 5. Conclusions are summarized in Section 6. The simple analytic constraint on secular variation is derived in Appendix A and the remade GSFC(9/80) field model, designated GSFC(10/84), is presented in Appendix B.

2. Frozen-Flux Constraints for Geomagnetic Field Modeling

A plausible first model for the coupled electromagnetism and fluid dynamics of the Earth's core can be based upon the following simplifying assumptions:

1) the core fluid is inviscid, incompressible, perfectly conducting, and its magnetic permeability is that of vacuum
2) the CMB is a smooth sphere (of radius r=b) everywhere on which vertical fluid motion vanishes
3) unsteady change in vertical absolute vorticity of fluid adjacent to the CMB is produced only by Coriolis and inertial torques (i.e. baroclinic, Lorentz and viscous torques are ignored).

Under these assumptions, the vertical components of the induction equation and the absolute vorticity equation, when evaluated at the CMB, reduce to (Benton, 1985):

$$\frac{\partial B_r}{\partial t} + \frac{v}{b}\frac{\partial B_r}{\partial \theta} + \frac{w}{b\sin\theta}\frac{\partial B_r}{\partial \phi} = B_r \frac{\partial u}{\partial r}, \qquad (2)$$

$$\frac{\partial \xi'}{\partial t} + \frac{v}{b}\frac{\partial \xi'}{\partial \theta} + \frac{w}{b\sin\theta}\frac{\partial \xi'}{\partial \phi} = \xi' \frac{\partial u}{\partial r}. \qquad (3)$$

Here u, v, w are the vertical, southward, eastward components of motion and ξ' is the vertical component of absolute vorticity, i.e.

$$\xi' = \hat{r} \cdot \nabla \times (\vec{v} + \vec{\Omega} \times \vec{r}) \qquad (4)$$

where $\vec{v}$ is the fluid velocity vector relative to the mantle and $\vec{\Omega}$ is the angular velocity of the earth (assumed constant on the short time scales of interest here). Benton (1985) notes the existence of four classes of conserved magnetic or vorticity flux integrals that result from this physical model:

$$\iint_{S_M} B_r \, dS = \text{constant} \tag{5}$$

$$\iint_{S_V} B_r \, dS = \text{constant} \tag{6}$$

$$\iint_{S_M} \xi' \, dS = \text{constant} \tag{7}$$

$$\iint_{S_V} \xi' \, dS = \text{constant} \tag{8}$$

where S_M and S_V denote area patches on the CMB bounded by null-flux curves (where $B_r = 0$) and "null-spin curves" (where $\xi' = 0$). Here, equation (5) results from assumptions (1) and (2) above, whereas (8) results from assumptions (2) and (3); all three assumptions are needed to derive (6) and (7).

The total number of independent constraints that emerge from these integrals is quite large. For example, if N_1, N_2 are, respectively, the number of distinct null-flux curves and null-spin curves on the CMB, then one obtains $2N_1$ constraints from eqs. (5) and (7) and $2N_2$ constraints from eqs. (6) and (8) (where it may be noted that N_1 null-flux curves divide the CMB into N_1+1 distinct "magnetic patches," S_M; but because the total magnetic flux across the entire CMB vanishes in the absence of monopoles, the number of independent

magnetic constraints is just N_1; a similar result follows for the null-spin curves, because absolute vorticity is a solenoidal vector). Benton (1985) notes further that in all likelihood vertical absolute vorticity is strongly dominated by planetary vorticity, $2\vec{\Omega}$, everywhere at the top of the core. Then there is only one null-spin curve (N_2=1), the "absolute vorticity equator," and it nearly coincides with the geographic equator. Two interesting consequences of this are first that north-south fluid motion vanishes at the geographic equator in this model

$$v = 0 \quad \text{on } r = b \quad \text{at } \theta = \frac{\pi}{2} \text{ for all } \phi, t \ , \tag{9}$$

and secondly, that intersections of the main magnetic and absolute vorticity equators, say N_3 in number, contribute a further N_3 boundaries of mixed type for area patches that move with the fluid and therefore conserve the magnetic and absolute vorticity flux enclosed by them. Each such mixed patch is the area bounded by a segment of the geomagnetic equator and the absolute vorticity equator between two successive intersections of those two curves. If the velocity potential and stream function for the surface fluid motion of the core are each expanded in spherical harmonics to truncation level N_4 (Voorhies, 1984), then eq. (9) provides $2N_4+1$ independent constraints on the resulting

velocity coefficients. In toto then, we have a total of N_c independent constraints, where

$$N_c = 2(N_1+N_2+N_3+N_4) + 1 \quad . \tag{10}$$

For typical numerical values we have $N_1=8$, $N_2=1$, $N_3=6$, $N_4=8$ giving $N_c=47$.

In this paper we have selected five constraints of the form of eq. (5) from this larger set to incorporate into a field model. Equation (5) expresses conservation of magnetic flux through magnetic patches on the CMB. Because the boundary of each such integral is a null-flux curve on which $B_r = 0$, there is locally zero contribution to each integral just at its boundary. Nonetheless, the boundary location is a highly non-linear function of the model parameters (taken here as Schmidt quasi-normalized Gauss coefficients because we assume the mantle to be an insulator). Consequently, these magnetic constraints are non-linear and an iterative approach is adopted.

Another independent constraint, based upon (6), is useful for assessing the constrained models. Conservation of total (not absolute) magnetic flux through the northern geographic hemisphere of the CMB is shown in Appendix A to be expressible as a simple, linear analytic constraint on the zonal Gauss coefficients of odd degree (Chapman and Bartels, 1940):

$$\frac{1}{2\pi(a/b)^3} \int_0^{2\pi}\int_0^{\pi/2} \frac{\partial B_r}{\partial t} \sin\theta d\theta d\phi = \sum_{n=1}^{N} F_n \dot{g}_n^{o}(t) = 0 \tag{11}$$

where $F_0 = 0$, $F_1 = 1$, $F_{n+2} = -n(n+1)^{-1}(a/b)^2 F_n$ for $n = 0, 1, 2 \ldots$. Here, $a = 6371.2$ km is the mean radius of the Earth and $\dot{g}_n^0$ is the zeroth order secular variation coefficient of degree n. The first seven non-zero terms of this constraint take the form

$$\dot{g}_1^0 - \frac{1}{2}\left(\frac{a}{b}\right)^2 \dot{g}_3^0 + \frac{3}{8}\left(\frac{a}{b}\right)^4 \dot{g}_5^0 - \frac{5}{16}\left(\frac{a}{b}\right)^6 \dot{g}_7^0 + \frac{35}{128}\left(\frac{a}{b}\right)^8 \dot{g}_9^0 - \frac{63}{256}\left(\frac{a}{b}\right)^{10} \dot{g}_{11}^0 + \frac{231}{1024}\left(\frac{a}{b}\right)^{12} \dot{g}_{13}^0 = 0 \qquad (12)$$

This model therefore predicts that the present rapid decay rate of the axial dipole moment of the Earth should show up as enhanced excitation of the weighted odd degree zonal harmonics of secular variation.

3. Least Squares Parameter Estimation with Non-Linear Constraints

The Bayesian parameter estimation algorithm provides a methodology for including a priori statistical information on the parameter space in obtaining least squares solutions (Luenberger, 1973). Let x denote the parameter vector, y the measurement vector and ν the random noise vector with zero mean and covariance matrix R. Then the observation equation is

$$y = F(x) + \nu \ . \qquad (13)$$

In the linear case, $F(x) = Ax$ so that

$$y = Ax + \nu \ . \qquad (14)$$

Then if $\hat{x}_a$ denotes an a priori estimate of the parameters with a priori

covariance matrix Ω_a, the estimate for the parameter state vector $\hat{x}$ is

$$\hat{x} = (A^T R^{-1} A + \Omega_a^{-1})^{-1} [A^T R^{-1} y + \Omega_a^{-1} \hat{x}_a] \quad . \tag{15}$$

This result may be obtained by minimizing, with respect to $\hat{x}$, the least squares norm J_{LS}, where

$$J_{LS}(x) = (y-Ax)^T R^{-1}(y-Ax) + (x-\hat{x}_a)^T \Omega_a^{-1} (x-\hat{x}_a) \quad . \tag{16}$$

It is clear that the a priori information is included in the formalism as additional data.

For the non-linear problem, an iterative approach is required. Linearizing about a nominal solution x_0, we have

$$F(x) - F(x_0) = A(x_0)(x-x_0) + \ldots \quad . \tag{17}$$

A Gauss iteration procedure yields the equation for the $(n+1)^{st}$ approximation to the solution estimate where

$$\hat{x}_{n+1} = x_n + \delta\hat{x}_{n+1} \tag{18}$$

$$\delta\hat{x}_{n+1} = (A^T(\hat{x}_n) R^{-1} A(\hat{x}_n) + \Omega_a^{-1})^{-1} [A^T(\hat{x}_n) R^{-1} \delta y_n + \Omega_a^{-1} [\hat{x}_a - \hat{x}_n]]$$

and

$$\delta y_n = y - A(\hat{x}_n)\, \hat{x}_n \quad .$$

The rate of convergence of the procedure depends on how good the nominal

guess x_0 is, and on the non-linear character of the function F(x). For highly non-linear problems, other techniques utilizing higher order derivatives may be required.

The implementation of constraints may be accomplished within the estimator formalism by Lagrange multiplier techniques (see Gubbins, 1984) or by considering the constraint equations to be data. If a non-linear constraint equation is represented as

$$G(x) = g \tag{19}$$

then the $(n+1)^{st}$ iteration relation is

$$\delta\hat{x}_{n+1} = [A^T(\hat{x}_n)\, R^{-1}\, A(\hat{x}_n) + \Omega_a^{-1} + C^T(\hat{x}_n)\, R_c^{-1}\, C(\hat{x}_n)]^{-1}$$

$$\cdot [A^T(\hat{x}_n)\, R^{-1}\, \delta y_n + \Omega_a^{-1}(\hat{x}_a - \hat{x}_n) + C^T(\hat{x}_n)\, R_c^{-1}\, \delta g_n] \tag{20}$$

where

$$C(\hat{x}_n) = \frac{\partial G}{\partial x}\Big|_{\hat{x}_n} \tag{21}$$

$$\delta g_n = g - C(\hat{x}_n)\hat{x}_n \quad .$$

The weight matrix R_c^{-1} reflects the stiffness of the constraint, where R_c is the "covariance" matrix of the "observed" constraint. This error measure may be chosen to represent the estimated numerical precision lost in the computing process, or to represent modeling errors inherent in the constraint. This result is obtained by minimizing the least squares norm

$$J_{LS} = \delta y_n^T R^{-1} \delta y_n + (\hat{x}-\hat{x}_a)^T \Omega_a^{-1} (\hat{x}-\hat{x}_a) + \delta g_n^T R_c^{-1} \delta g_n \quad , \qquad (22)$$

This approach has also been taken by Bloxham and Gubbins (1985).

In the absence of constraints, the least squares estimation process converges rapidly (in usually no more than two iterations) when the time dependence of Gauss coefficients is a power series. In that representation, the observations of magnetic components X, Y, Z, are linear functions of the Gauss coefficients whereas the scalar field intensity, horizontal field, declination, and inclination are nonlinear functions of those parameters. While the measurements will be nonlinear functions of the parameters, they are at least, still represented in analytic form. In contrast, most of the frozen-flux constraints are not available in analytic form. For example, the null-flux curves on which the vertical magnetic field vanishes are extremely complex functions of the model parameters and must be determined numerically. As a result numerical methods have been used to compute the matrix

$$C^T(\underline{x}_n)C(\underline{x}_n)$$

for each iteration, n = 0,1,2, ... , until convergence was approached.

4. Derivation of a Field Model Constrained by Flux Conservation

To investigate the influence of frozen-flux constraints on geomagnetic field models, we now apply the non-linear algorithm described in Section 3 to a

variation of the GSFC(12/83) field model (Langel and Estes, 1985). That model utilized quiet, scalar and vector MAGSAT data and annual means from a selected set of observatories for the years 1977 through 1982. Internal main field and secular variation Gauss coefficients were included to order and degree 13 and 10, respectively. The degree one external harmonics were also retained and vector biases were calculated for each observatory. Moreover, the internal axial dipole coefficient and the external coefficients were corrected for linear Dst variation. However, those internal coefficients which were not determined by the data inversion to the 95% confidence level were forced to be zero in the final solution. Because the incorporation of dynamic constraints from the core could improve the observability of such suppressed coefficients, the GSFC(12/83) model has now been recomputed with all of the above coefficients retained in the solution and with all partial derivatives included in the normal equations matrix, $A^T R^{-1} A$. This starting model is designated GSFC(9/84-0). The number of obervatories (by year) used in GSFC(9/84-0) is 86 (1977.5), 91 (1978.5), 90 (1979.5), 90 (1980.5), 45 (1981.5), 8 (1982.5).

The GSFC(9/84-0) field model, utilizing high quality MAGSAT data, represents the geomagnetic field at and above the Earth's surface very accurately at epoch 1980.0. Figure 1 displays its radial component at the core-mantle boundary at 1980.0, using all Gauss coefficients to order and degree 13. This model has ten distinct null-flux curves, all but two of which

(one near the north pole and one beneath the eastern North Pacific) also appear in the recent stochastic inversion model at 1980 constructed by Bloxham and Gubbins (1986). Because the high degree Gauss coefficients, which are less well determined, multiply spherical harmonics that become more dominant at the CMB than at the Earth's surface, such computations become subject to large uncertainty. Benton et al. (1982) examined the effect of varying the spherical harmonic truncation level, N, on geomagnetic properties at the CMB, finding considerable dependence in null-flux curve location and included magnetic flux. In this work we have therefore selected only five null-flux curves for which to impose the constraints. Those five, labeled in Figure 1, are present in the model of Gubbins and Bloxham (1986), and are also reasonably stable features of the magnetic maps at the CMB prepared by Benton et al. (1979) for N ranging from 9 to 12.

The methodology for computing magnetic flux through each null-flux curve (whose enclosed area is referred to as a null-flux patch, Backus, 1968) is to overlay a 1° x 1° grid and then to approximate the field within each 1° x 1° cell by its value at the center. The required partial derivatives with respect to the model parameters were also determined numerically for each cell by varying the nominal Gauss coefficient value. We note that the magnetic flux through null-flux patches depends upon both main field and secular variation coefficients because the integrand, B_r, and boundary of integration, the

null-flux curves, each vary with time.

For each of the five selected null-flux patches, the constraints are imposed at epochs 1977.5, 1980.0 and 1982.5 in the form of equation (5) with the constants set to the values obtained from the GSFC(9/84-0) model at 1980.0. We are therefore adding 15 nonlinear constraints to the GSFC(9/84-0) data set in such a way as to force conservation of magnetic flux through those five null-flux patches. The elements of the diagnonal weight matrix R_c^{-1} were set to represent an error measure of 10^{-5} MWb on the "observed flux," this value being selected (by numerical experimentation) to provide a stable inversion of the normal equations matrix.

The solution was advanced through three iterations using equation (20), starting with the GSFC(9/84-0) model as the nominal parameter vector for iteration number one. No a priori information was assumed for the nominal model, so Ω_a^{-1} is zero in equation (20). Each iteration was performed in two stages. First, the MAGSAT and observatory data set published for the GSFC(12/83) model were processed and the normal equations matrix, $A^T(\hat{x}_n)R^{-1}A(\hat{x}_n)$ and the vector $A^T(\hat{x}_n)R^{-1}\delta y_n$ were accumulated. From this information an "unconstrained" model was generated for each iteration, they

are designated GSFC(9/84-1), GSFC(9/84-2), and GSFC(9/84-3) for iterations one, two and three, respectively. Note that for iteration one, GSFC(9/84-1) is identical to GSFC(9/84-0) because the latter had already converged from the GSFC(12/83) data set. In the second stage of each iteration, the flux and its partial derivatives for the fifteen observation equations were computed and the matrix $C^T(\hat{x}_n)R_c^{-1}C(\hat{x}_n)$ and the vector $C^T(\hat{x}_n)R_c^{-1}\delta g_n$ were formed and then added to the first stage quantities. The "constrained" models so obtained are denoted as GSFC(9/84-1C), GSFC(9/84-2C) and GSFC(9/84-3C) for iterations one, two and three respectively. The final constrained model is also referred to simply as GSFC(9/84).

5. Assessment of the Flux-Constrained Geomagnetic Field Model, GSFC(9/84)

Table 1 has been prepared to reveal how well or poorly the various iterative models satisfy the imposed constraints. The model name is given in the first column, followed by the epoch (in years beyond 1900). The first three entries of the third column give the magnetic flux (in MWb) through null-flux patch number one at the three epochs indicated whereas the offset number (-6.9) is the rate of change of flux (in MWb/yr) at 1980. The maximum variation in flux (in MWb) between a single model at the three epochs is listed in the fourth column. The final column gives the root sum square flux rate (in MWb/yr) for all five null-flux patches. For a perfectly constrained solution,

the flux values at each epoch for each single null-flux patch would coincide and the flux rates would be zero. Table 1 shows a trend towards reduced total flux variation for the five year data interval as the model converges. The poorest improvement is for the extreme southern null-flux patch number 2, whose initial 5 year maximum flux variation of 30 MWb is reduced to 19 MWb after three iterations. The constraints are clearly strongly felt with the other four null-flux patches. For all five patches the root sum square flux rate at 1980 is reduced from 16.1 MWb/yr to 5.9 MWb/yr as the iterations proceed.

Because the unconstrained solutions are optimum in the least squares sense, the imposition of constraints must degrade the fit to the data. To examine the amount of this degradation we consider the cost function, J_{LS}, being minimized by the estimation procedure. With equation (22) written in the form $J_{LS} = \delta y_n^T R^{-1} \delta y_n + \delta g_n^T R_c^{-1} \delta g_n$ its first term represents the weighted sum of the squares of the model misfits to the MAGSAT and observatory data, now designated by Q. Table 2 presents the values of Q for the two data types separately, as well as in toto, and for the observatory data, the Q values are shown for each magnetic field component, X,Y,Z separately. As expected, the inclusion of constraints increases the misfit, but by less than one percent overall, for the final iteration. Although the solution appears to have converged with respect to the massive set of MAGSAT data used, the situation

is less clear with respect to the observatory data. This probably reflects the fact that the constraints affect the fit to secular variation (i.e. observatory data) more strongly than they affect the fit to the short span of MAGSAT data. For completeness, Table 2 also lists the root mean square of the residuals of the various models to all of the MAGSAT data (in the third column) and to the three components of the observatory data (in the fifth column). This again shows that imposing these constraints only causes the misfit to the data (in terms of residuals) to grow slightly.

A stringent test, both of the frozen-flux approximation and the utility of including the resulting physical constraints into geomagnetic field models, is provided by comparing how well or poorly unconstrained and constrained models predict the magnetic field evolution when they are extrapolated beyond the data interval that defined the models. The results of this test are displayed in Figures 2-5 which are, respectively, temporal plots of the root mean square residuals of the X,Y,Z magnetic field compoonents, and the scalar intensity, $B = (X^2+Y^2+Z^2)^{1/2}$. Here X,Y,Z are the northward, eastward and downward components and the residuals are the differences between the anual means data and model values at the number of observatories indicated beneath the dates along the abscissa. The observatory biases calculated for each model were used in computing these statistics and the standard deviations are plotted with a different symbol for each model. Within the resolution available

on these plots the points for GSFC(9/84-3) and GSFC(9/84-3C) coincide, respectively, with those for GSFC(9/84-2) and GSFC(9/84-2C) so they are not displayed separately. The vertical bars crossing the abscissa at 1977.5 and 1981.5 delineate the primary 4 year interval for observatory data. The dashed vertical line at 1982.5 is to emphasize that only 8 observatories contributed to the solution at that epoch so the statistics for 1982.5 are most indicative of predictive errors. Because only nine observatories contributed to the standard deviation at 1984.5 it must be considered unreliable.

Figures 2-5 generally reveal that the final constrained model is in better agreement with observatory data when extrapolated 2 years, either forward or backward, outside the primary data interval 1977.5-1981.5. The reduction in root mean square residual is more pronounced in the relatively poorly predicted vertical component, Z (Figure 4) than in the horizontal components. For example, σ_Z at 1975.5 for constrained model GSFC(9/84-2C) is only about 75% of that for unconstrained model GSFC(12/83). The improvement in the Y component (Figure 3) is not dramatic, but those residuals are uniformly smaller anyway, than for the X and Z component. The standard deviation in field intensity, Figure 5, is reduced by up to about 20% by imposition of the constraints.

Because the predictability of Z is enhanced most, and that is the component needed for extrapolation to the core-mantle boundary in studies

designed to evaluate the fluid motions just beneath the CMB, these findings are viewed as encouraging. It should be noted that the improved prediction capability has been achieved without altering the mathematical form of the secular variation model.

A different test of these constrained models is provided by asking whether they also satisfy other independent theoretical frozen-flux constraints, specifically the one arising from consideration of vorticity dynamics as discussed in Section 2 and Appendix A. Because the validity of that constraint has not yet been firmly established, we first derived a new field model, designated GSFC(10/84) which is totally free of all frozen-flux constraints. This model, essentially a remake of the GSFC(9/80) field model, is described and documented in Appendix B.

The possibility that the secular variation coefficients of this model satisfy the theoretical constraint given in equations (11) and (12) is examined in Figure 6. The normalized flux of secular variation out of the northern geographic hemisphere is plotted versus degree of spherical harmonic for three epochs well within the 1960-1982 data interval used for the model. As higher odd degree zonal harmonics are successively added, the cumulative sum in equation (11) or (12) does indeed appear to approach zero. This model appears to satisfy the constraint exactly at some epoch shortly after 1970, i.e. very close to the centroid of the data used.

Having established that GSFC(10/84) supports flux conservation through the northern geographic hemisphere for a decade or so, we now ask whether the other models introduced in this paper tend to obey or to violate this constraint. Table 3 lists the axial dipole coefficient decay rate, g_1^0 in nT/yr, i.e. the first term in equation (12), as well as the cumulative sum of all the terms in (12) for six different field models, evaluated at 1980 (the center of their data intervals).

When compared with the results in Figure 6, we find that the final constrained model, GSFC(9/84-3C) also conserves very well the northern hemispheric magnetic flux crossing the CMB. It might be argued that this must follow because conservation of magnetic flux southward of the magnetic equator in null-patch number 1 of Figure 1 was impressed as a constraint in that model. However, that reasoning is not justified for two reasons. Firstly, the southern geographic total hemispheric magnetic flux (equal and opposite to that considered in arriving at equations 11, 12) differs, by about 9%, from the absolute magnetic flux southward of the magnetic equator, and furthermore, the flux in null-flux patch 2 was not strongly conserved in the three iterations calculated herein. Thus, there is room for the GSFC(9/84-3C) model to violate this constraint, should the data warrant it.

Readers interested in obtaining the Gauss coefficients of this model may obtain them from R.H. Estes.

6. Conclusion

This paper has introduced into geomagnetic field modeling a selected set of highly nonlinear constraints that arise from the frozen-flux theory of electromagnetism for the earth's core. Forcing magnetic flux through five null-flux patches to be driven toward the same values at each of three slightly different epochs (1977.5, 1980.0, 1982.5) adds fifteen constraints to the satellite and observatory data bases that define the models. The constraints are incorporated like data in an iterative Bayesian parameter estimation procedure that approaches convergence after three iterations.

The final constrained model, GSFC(9/84), has been tested by examining the temporal growth of its residuals to observatory data during the two year intervals that precede and follow the span of data that defined the model. This stringent test was passed favorably in the sense that the constrained model was found to be a somewhat better hindcaster and forecaster of the time evolution of the geomagnetic field (especially the vertical component) than is the unconstrained model used to start the iterative modeling algorithm. Also, the imposition of the constraints caused the misfit between the model and the satellite and observatory data to grow only slightly.

Another longer duration field model, totally unconstrained by flux conservation, has also been developed and presented as an improvement to the recent GSFC(9/80) field model. This model is found to have a secular variation

component which maintains, for a decade, nearly a null value for the flux of geomagnetic secular variation out of the northern geographic hemisphere of the core-mantle boundary, in accordance with a recent theoretical prediction of Benton (1985). The new constrained model was then examined and it too appears to satisfy this independent constraint.

We conclude that the incorporation into short duration geomagnetic field models of constraints arising from the frozen-flux theory of the earth's core is both feasible and of some predictive value. It remains to be determined by how much the data interval defining the models and constraints can be lengthened and also whether the inclusion of more constraints that are available will sustain the above conclusion.

Acknowledgements

The work of ERB reported here has been supported, in part, at the University of Colorado by NSF Grant EAR-7926120 and NASA Contracts NAS5-27671 and NAS5-28617 as well as at the U.S. Geological Survey, Denver, Colorado. RHE has been supported by NASA Contracts NAS5-27672 and NAS5-28671 to his former employer, Business and Technological Systems, Inc. The authors are grateful to the funding agencies and to the above institutions where this work was completed..

References

Backus, G.E., 1968. Kinematics of geomagnetic secular variation in a perfectly conducting core. Philos. Trans. R. Soc. (London), Ser. A, 263: 239-266.

Backus, G.E. and LeMouel, J.-L., 1986. The region on the core-mantle boundary where a geostrophic velocity field can be determined from frozen-flux magnetic data. Geophys. J. Roy. Astron. Soc., in press.

Benton, E.R., 1979a. On fluid circulation around null-flux curves at Earth's core-mantle boundary. Geophys. Astrophys. Fluid Dyn., 11: 323-327.

Benton, E.R., 1979b. Magnetic probing of planetary interiors. Phys. Earth Planet. Inter. 20:111-118.

Benton, E.R., 1981a. A simple method for determining the vertical growth rate of vertical motion at the top of Earth's outer core. Phys. Earth Planet. Inter., 24: 242-244.

Benton, E.R., 1981b. Inviscid, frozen-flux velocity components at the top of Earth's core from magnetic observations at Earth's surface, Part 1. A new methodology. Geophys. Astrophys. Fluid Dyn., 18: 157-174.

Benton, E.R., 1985. On the coupling of fluid dynamics and electromagnetism at the top of the Earth's core. Geophys. Astrophys. Fluid Dyn., 33: 315-330.

Benton, E.R. and Muth, L.A., 1982. Sensitivity of selected geomagnetic properties to truncation level of spherical harmonic expansions. Geophys. Res. Lett., 9: 254-257.

Benton, E.R. and Muth, L.A., 1979. On the strength of electric currents and zonal magnetic fields at the top of Earth's core: Methodology and preliminary estimates. Phys. Earth Planet. Inter., 20: 127-133.

Benton, E.R., Muth, L.A., and Stix, M., 1979. Magnetic contour maps at the core-mantle boundary. J. Geomag. Geoelectr., 31: 615-626.

Bloxham, J. and Gubbins, D., 1985. The secular variation of the Earth's magnetic field. Nature, 317: 777-781.

Bloxham, J. and Gubbins, D., 1986. Geomagnetic field analysis--IV. Testing the frozen-flux hypothesis. Geophys. J. Roy. Astron. Soc., 84: 139-152.

Bondi, H. and Gold, T., 1950. On the generation of magnetism by fluid motion. Mon. Not. R. Astron. Soc., 110: 607-611.

Booker, J.R., 1969. Geomagnetic data and core motions. Proc. R. Soc. (London), Ser. A, 309: 27-40.

Chapman, S. and Bartels, J., 1940. Geomagnetism, Volume II, Oxford University Press.

Gubbins, D., 1982. Finding core motions from magnetic observations. Philos. Trans. R. Soc. (London), Ser. A., 306: 247-254.

Gubbins, D., 1983. Geomagnetic field analysis--I. Stochastic inversion. Geophys. J. Roy. Astron. Soc., 73: 641-652.

Gubbins, D., 1984. Geomagnetic field analysis--II. Secular variation consistent with a perfectly conducting core. Geophys. J. Roy. Astron. Soc., 77:

753-766.

Gubbins, D. and Bloxham, J., 1985. Geomagnetic field analysis--III. Magnetic fields on the core-mantle boundary. Geophys. J. Roy. Astron. Soc., 80: 695-713.

Gubbins, D. and Roberts, N., 1983. Use of the frozen flux approximation in the interpretation of archaeomagnetic and palaeomagnetic data. Geophys. J. Roy. Astron. Soc., 73: 675-687.

Hide, R., 1978. How to locate the electrically conducting fluid core of a planet from exernal magnetic observations. Nature, 271: 640-641.

Hide, R. and Malin, S.R.C., 1981. On the determination of the size of the Earth's core from observations of the geomagnetic secular variation. Proc. R. Soc. (London), Ser. A, 378: 15-33.

Langel, R.A. and Estes, R.H., 1985. The near-Earth magnetic field at 1980 determined from Magsat data. J. Geophys. Res., 90: 2495-2509.

Langel, R.A., Estes, R.H., and Mead, G.D., 1982. Some new methods in geomagnetic field modeling applied to the 1960-1980 epoch. J. Geomagn. Geoelectr., 34: 327-349.

LeMouel, J.-L., Gire, C. and Madden, T.R., 1986. Motions at the core surface in the geostrophic approximation. Geophys. J. Roy. Astron. Soc., in press.

Luenberger, D.G., 1973. Introduction to Linear and Nonlinear Programming. Addison-Wesley Publishing Co., Reading Mass.

Madden, T.R. and LeMouel, J.-L., 1982. The recent secular variation and motions at the core surface. Philos. Trans. R. Soc. (London) Ser. A, 306: 271-280.

Roberts, P.H. and Scott, S., 1965. On analysis of the secular variation. 1. A hydromagnetic constraint: theory. J. Geomag. Geoelectr., 17: 137-151.

Shure, L., Whaler, K.A., Gubbins, D. and Hobbs, B., 1983. Physical constraints for the analysis of the geomagnetic secular variation. Phys. Earth Planet. Inter., 32: 114-131.

Voorhies, C.V., 1984. Magnetic location of earth's core-mantle boundary and estimates of the adjacent fluid motion. Unpublished Ph.D. Thesis, University of Colorado, Boulder, Colorado, 350 pages.

Voorhies, C.V. and Backus, G.E., 1985. Steady flows at the top of the core from geomagnetic field models: The steady motions theorem. Geophys. Astrophys. Fluid Dyn., 32: 163-173.

Voorhies, C.V. and Benton, E.R., 1982. Pole-strength of the earth from MAGSAT and magnetic determination of the core radius. Geophys. Res. Lett., 9: 258-261.

Whaler, K.A., 1980. Does the whole of the Earth's core convect? Nature, 287: 528-530.

Whaler, K.A., 1982. Geomagnetic secular variation and fluid motion at the core surface. Philos. Trans. R. Soc. (London), Ser. A, 306: 235-246.

Whaler, K.A., 1984. Fluid upwelling at the core-mantle boundary--resolvability

from surface geomagnetic data. Geophys. J. Roy. Astron. Soc., 78: 453-473.

Figure Captions

Figure 1: Contour map of the downward vertical magnetic field on the Earth's core-mantle boundary at epoch 1980.0 according to the GSFC(9/84-0) field model. Small numerals are field values (in gauss) for each contour. Large numerals (1 through 5) are labels for null-flux patches.

Figure 2: Variation of σ_X with time (unweighted) for observatory annual means including model anomalies.

Figure 3: Variation of σ_Y with time (unweighted) for observatory annual means including model anomalies.

Figure 4: Variation of σ_Z with time (unweighted) for observatory annual means including model anomalies.

Figure 5: Variation of σ_B with time (unweighted) for observatory annual means including model anomalies.

Figure 6: Normalized flux of secular variation through the northern geographic hemisphere of the core-mantle boundary

$$\left(\frac{1}{2\pi(a/b)^3}\int_0^{2\pi}\int_0^{\pi/2}\frac{\partial B_r}{\partial t}\sin\theta\, d\theta\, d\phi,\ \text{in nT/yr}\right)$$

as a function of spherical harmonic degree according to the GSFC(10/84) field model.

TABLE 1. SOLUTION FLUX AND FLUX RATE THROUGH NULL CURVES
MWb AND MWb/YR

MODEL	EPOCH	NULL CURVE	PATCH 1	MAX VARIATION |Δ|	PATCH 2	MAX VARIATION |Δ|	PATCH 3	MAX VARIATION |Δ|	PATCH 4	MAX VARIATION |Δ|	PATCH 5	MAX VARIATION |Δ|	RSS of Flux Rate
GSFC 9/84-0													
Flux	77.5		-17454		1410		156		-37		53		
	80.0		-17449		1386		131		-56		40		
	82.5		-17488		1380		107		-77		32		
Flux Rate	80.0		-6.9	39	-5.7	30	-10.0	49	-8.0	40	-3.8	21	16.1
GSFC 9/84-1C													
Flux	77.5		-17456		1408		133		-56		41		
	80.0		-17443		1391		127		-52		38		
	82.5		-17472		1405		133		-56		40		
Flux Rate	80.0		-2.4	29	-0.1	17	-0.1	6	-0.2	4	-0.1	.3	2.4
GSFC 9/84-2													
Flux	77.5		-17448		1408		142		-38		54		
	80.0		-17440		1392		128		-55		40		
	82.5		-17452		1388		119		-74		28		
Flux Rate	80.0		-0.6	12	-3.8	20	-4.6	23	-7.4	36	-5.4	26	10.9
GSFC 9/84-2C													
Flux	77.5		-17453		1400		125		-47		42		
	80.0		-17444		1390		128		-54		42		
	82.5		-17437		1396		133		-62		44		
Flux Rate	80.0		5.5	16	-1.0	10	1.8	8	-3.2	15	0.5	2	6.7
GSFC 9/84-3													
Flux	77.5		-17448		1408		141		-38		54		
	80.0		-17439		1392		129		-55		40		
	82.5		-17451		1388		118		-74		27		
Flux Rate	80.0		-0.7	12	-3.8	20	-4.7	23	-7.4	36	-5.5	27	11.0
GSFC 9/84-3C													
Flux	77.5		-17436		1405		127		-61		40		
	80.0		-17438		1389		130		-56		41		
	82.5		-17450		1386		136		-54		41		
Flux Rate	80.0		-4.0	14	-3.7	19	1.9	9	1.3	7	0.2	1	5.9

TABLE 2. COST FUNCTION EVALUATION

MODEL	MAGSAT (54,813 OBSERVATIONS)		OBSERVATORY (972 OBSERVATIONS)		TOTAL Q
	Q	RMS OF ALL DATA RESIDUALS (nT)	Q	RMS OF X, Y, Z RESIDUALS (nT)	
GSFC 984-0	22,332	6.38	5891	14.3 4.6 5.9	28,223
GSFC 984-2	20,916	6.17	5605	14.1 4.6 5.4	26,521
GSFC 984-2C	21,065	6.20	5799	14.3 4.5 5.7	26,864
GSFC 984-3	20,916	6.17	4239	11.2 4.5 6.2	25,155
GSFC 984-3C	21,060	6.19	4309	11.0 4.6 6.6	25,369

TABLE 3. COMPLIANCE OF VARIOUS FIELD MODELS WITH LINEAR ANALYTIC CONSTRAINT ON SECULAR VARIATION COEFFICIENTS

Model Name	Secular Variation of the Axial Dipole Coefficient g^0_1(nT/yr)	Normalized Flux of Secular Variation Out of Northern Hemisphere of the CMB, in nT/yr
GSFC(12/83)	26.5	-1.9
GSFC(9/84-0)	26.3	-6.2
GSFC(9/84-2)	24.8	-2.0
GSFC(9/84-2C)	24.9	6.0
GSFC(9/84-3)	24.8	-2.0
GSFC(9/84-3C)	24.9	0.6

TABLE 4. GAUSS COEFFFICIENTS FOR GSFC (10/84) AT EPOCH 1980. UNITS IN nT

N	M	g_{nm}	h_{nm}	g_{nm}	h_{nm}	$\dot{g}_{nm}$	$\dot{h}_{nm}$	$\ddot{g}_{nm}$	$\ddot{h}_{nm}$
1	0	-29992 10	0.00	20 833	0 000	-0.6521	0.0000	-0 07241	0 00000
1	1	-1955.70	5603 90	10.772	-15 973	-0.1948	-0.4694	-0 02893	0 03138
2	0	-1996.60	0.00	-17.773	0 000	1.0521	0.0000	0 08398	0.00000
2	1	3027.40	-2129 00	4.084	-16.152	0 3539	-2.2172	0 01536	-0.22115
2	2	1662 50	-199.46	5.624	-26 477	0 1224	-0.8740	-0 01135	-0 03275
3	0	1281.10	0.00	3.362	0 000	1.2284	0.0000	0.12058	0.00000
3	1	-2180.70	-334 93	-4.301	-0 126	1.1791	-0.9699	0 09956	-0.07104
3	2	1250.80	271.21	-0 658	1 935	0.7282	-0.1680	0.08857	-0.02257
3	3	832.63	-252.73	2.110	-7 061	0.8154	-0 6155	0 05543	-0.07826
4	0	937.47	0.00	-2.186	0 000	-0 1665	0.0000	-0.01000	0.00000
4	1	782 39	212.53	-1.110	3 099	0 1730	-0.3269	0.02415	-0.04263
4	2	397 85	-256.42	-9 012	1 395	-0.7660	0.0755	-0 05721	0.00602
4	3	-418.89	53 10	-2 509	4 228	0 0530	0.5049	0 02582	0 05363
4	4	198.36	-297 10	-5.399	-2.017	-0 5842	-0.2564	-0 06017	-0.04315
5	0	-218.15	0.00	-0.748	0 000	-0.1243	0.0000		
5	1	357.57	45 72	-0 649	2 406	-0 0660	0.0666		
5	2	260.98	149.98	-0 926	0.410	-0 2199	-0.1301		
5	3	-74 14	-150 56	-4 333	-0.722	-0.2173	0.1276		
5	4	-162.00	-77.67	-0 151	0 978	0 0072	-0.0420		
5	5	-48.10	92.06	0 547	0 961	-0.0342	0 0314		
6	0	47 89	0.00	0 986	0 000	0.1104	0.0000		
6	1	65.53	-14.69	-0.082	0.281	-0.0590	0.0760		
6	2	42.03	93.40	3 141	-1 176	0.1273	-0.0642		
6	3	-192 12	70.86	1 906	-0 410	-0 0544	-0.0772		
6	4	3.72	-43 21	0 432	-0 170	0.0476	0.0655		
6	5	13 92	-2 19	1.025	0.532	0 0341	0 0048		
6	6	-107.61	17.28	1 060	1.213	0 0955	-0.0403		
7	0	71 46	0 00	0 052	0 000				
7	1	-58.70	-83 07	-0 369	-1 352				
7	2	1.44	-27.34	0.047	-0.016				
7	3	20.52	-4 79	0.446	0 223				
7	4	-12 73	16 20	0.959	0 613				
7	5	0.67	17.87	0 403	-0 342				
7	6	10.64	-23 12	-0 298	0 091				
7	7	-1 67	-9 79	-0 161	0 403				
8	0	18.50	0 00	0 480	0 000				
8	1	6.72	6 97	0.097	-0 145				
8	2	-0.02	-17.58	0.193	-0 292				
8	3	-10.98	4 25	0.022	-0 085				
8	4	-7.05	-22.27	-0.243	-0.391				
8	5	4 19	9.26	-0.085	0 354				
8	6	2.86	16 13	0.417	-0 381				
8	7	6.35	-13 20	-0 348	-0 539				
8	8	-1 50	-14.90	-0.741	0.357				
9	0	4.96	0 00	-0 324	0 000				
9	1	10.51	-21.00	0.113	0.113				
9	2	1.18	16.01	-0.006	0.090				
9	3	-12.34	8.81	-0.002	0.252				
9	4	9 28	-4.94	-0.142	-0.127				
9	5	-3.61	-6.60	-0.345	-0.222				
9	6	-1 21	9.02	0.042	-0.057				
9	7	6 66	9.87	0.276	-0.049				
9	8	1 37	-5.68	-0.145	-0.386				
9	9	-5 00	2.20	-0.219	0.088				
10	0	-3.58	0.00	-0.116	0 000				
10	1	-3.93	0.94	-0.099	-0 094				
10	2	2 37	0.57	0.012	-0.021				
10	3	-5.21	2.58	-0.038	0.075				
10	4	-1.74	5.63	0.027	-0.011				
10	5	4.74	-4.42	-0.106	-0.047				
10	6	3.21	-0.45	-0.101	-0.045				
10	7	0.87	-1.35	0.049	0.007				
10	8	2.16	3.66	0 195	-0 007				
10	9	2.83	-0.57	-0 028	-0.112				
10	10	-0.05	-6 26	-0.104	-0.324				
11	0	2.45	0.00	0.017	0.000				
11	1	-0.89	0.71	0 016	-0.031				
11	2	-1.96	2.26	-0.004	-0.002				
11	3	2.01	-1.19	-0.155	0.067				
11	4	-0.11	-3.02	0 050	-0.042				
11	5	-0.65	0.88	-0 025	0 048				
11	6	-0.21	0.10	0 019	0 049				
11	7	1.47	-2.45	-0.011	-0 107				
11	8	1.75	-0.62	-0.026	-0 006				
11	9	-0.62	-1.55	0.056	0.070				
11	10	1.98	-1.38	-0.015	-0.066				
11	11	3.41	0.77	0.186	0.009				
12	0	-1.82	0.00	-0.021	0 000				
12	1	-0.21	0.07	-0.014	-0.046				
12	2	-0.02	0.73	0 076	0.007				
12	3	-0.07	2.47	0.010	0 003				
12	4	0.61	-1.39	-0 014	-0.084				
12	5	0 66	0.11	0 013	-0.014				
12	6	-0 75	0.15	-0.048	-0.023				
12	7	-0.19	-0.29	0 033	0.011				
12	8	0.42	0.06	0.032	-0.041				
12	9	-0.55	-0.04	-0.043	-0 026				
12	10	-0 03	-1.40	-0.024	0.022				
12	11	0 51	0.43	-0 009	-0.090				
12	12	0 19	0.41	0 029	-0 048				
13	0	-0 20	0.00	-0.050	0 000				
13	1	-0 44	-0.28	0.017	0.010				
13	2	0 00	0.44	-0.087	-0.020				
13	3	-0.71	1.62	0.014	0.047				
13	4	-0.10	-0.25	-0 033	-0 015				
13	5	0 90	-0.48	-0.007	-0.032				
13	6	-0 54	-0.11	-0.048	0.019				
13	7	0.35	0.94	0.022	0 056				
13	8	-0.42	0.14	0.013	0.020				
13	9	0.27	0.76	0.046	-0.010				
13	10	-0.16	-0.01	-0.006	0 015				
13	11	0.25	-0.08	-0.102	-0.033				
13	12	0.04	0.07	-0.012	-0 052				
13	13	0.41	-0.41	0.073	-0.210				

TABLE 5. NUMBER OF OBSERVATORIES USED IN GSFC (10/84) BY YEAR

YEAR	NUMBER OF OBSERVATORIES	YEAR	NUMBER OF OBSERVATORIES
1960.5	137	1971.5	157
1961.5	146	1972.5	154
1962.5	145	1973.5	156
1963.5	143	1974.5	156
1964.5	158	1975.5	153
1965.5	164	1976.5	149
1966.5	166	1977.5	145
1967.5	163	1978.5	141
1968.5	165	1979.5	139
1969.5	164	1980.5	118
1970.5	164	1981.5	73
		1982.5	17

TABLE 6
OBSERVATORIES AND BIAS SOLUTION

Observatory	Latitude (Deg)	Longitude (Deg)	Altitude (Km)	X Bias (nT)	Y Bias (nT)	Z Bias (nT)	Begin Year	End Year
ABISKO	68.36	18.82	0.37	38.0	56.9	34.6	1960.5	1980.5
ACACIAS	-35.01	-57.69	0.01	-8.9	2.7	12.8	1964.5	1978.5
ADAK	51.87	-176.64	0.0	-462.3	17.0	-96.7	1964.8	1966.0
ADDIS ABABA	9.03	38.76	2.44	495.7	5.9	117.0	1960.5	1980.5
AGINCOURT	43.78	-79.27	0.17	-15.5	166.4	-138.3	1960.5	1969.1
ALERT	82.50	-62.50	0.05	9.0	30.8	-142.2	1961.9	1980.5
ALIBAG	18.64	72.87	0.0	-91.8	449.0	672.2	1960.5	1977.5
ALIBAG II	18.64	72.87	0.0	-187.0	453.5	592.4	1978.5	1980.5
ALMA ATA	43.25	76.92	1.29	162.8	33.2	-181.8	1963.4	1981.5
ALMERIA	36.85	-2.46	0.06	2.9	21.7	3.3	1960.5	1980.5
AMATSIA	31.55	34.92	0.0	124.2	37.1	275.2	1976.5	1981.5
AMBERLEY II	-43.15	172.72	0.03	13.0	-6.8	89.2	1960.5	1977.5
ANNAMALAINAGAR	11.37	79.68	0.0	209.9	-82.4	-99.5	1960.5	1980.5
APIA III	-13.81	-171.77	0.0	-33.3	211.2	-919.1	1960.5	1980.5
AQUILA	42.38	13.32	0.62	12.5	39.5	-6.6	1960.5	1981.5
ARGENTINE ISLND	-65.24	-64.26	0.0	72.6	-76.2	494.5	1960.5	1982.5
ARTI	56.43	58.57	0.28	126.9	-265.9	448.0	1973.5	1981.5
BAKER LAKE	64.33	-96.03	0.04	170.0	-50.8	-99.4	1960.5	1968.5
BAKER LAKE II	64.33	-96.03	0.04	246.3	-136.8	-102.7	1969.5	1974.5
BAKER LAKE III	64.33	-96.03	0.04	176.8	-40.1	-87.8	1975.5	1980.5
BANGUI	4.44	18.57	0.38	-127.2	-65.7	171.6	1960.3	1965.5
BANGUI II	4.44	18.57	0.38	-63.3	1072.6	201.2	1966.5	1972.5
BANGUI III	4.44	18.57	0.38	-133.5	-44.9	210.3	1973.5	1982.5
BARROW II	71.30	-156.75	0.0	54.1	-58.5	69.3	1960.5	1962.5
BARROW III	71.32	-156.62	0.0	34.3	-62.2	-55.7	1963.5	1980.5
BEIJING	40.04	116.17	0.06	607.1	-224.9	406.7	1960.5	1980.5
BELSK	51.84	20.79	0.17	120.4	145.4	301.4	1960.5	1980.5
BEREZNAYKI	49.82	73.08	0.0	-390.5	8.5	314.4	1965.5	1976.5
BEREZNAYKI II	49.82	73.08	0.0	-356.6	-198.6	323.1	1977.5	1980.5
BINZA	-4.27	15.37	0.0	-80.7	-185.8	-50.3	1960.5	1973.5
BJORNOYA	74.50	19.20	0.07	-98.8	47.7	29.5	1960.5	1981.5
BOULDER	40.14	-105.24	1.64	-0.8	56.0	-166.3	1964.5	1980.5
BUDKOV	49.08	14.01	0.49	-25.6	-16.9	-32.5	1967.5	1978.5
BYRD II	-80.02	-119.52	1.51	-8.2	40.5	-137.7	1962.5	1968.3
CAMBRIDGE BAY	69.20	-105.00	0.01	108.9	-89.7	144.8	1972.5	1980.5
CANBERRA	-35.32	149.36	0.84	9.9	41.5	93.4	1979.5	1981.5
CASEY	-66.28	110.53	0.0	915.0	-311.7	-678.6	1978.5	1981.5
CASTELLACCIO	44.43	8.93	0.34	24.8	-197.1	-120.0	1960.5	1969.5
CASTLE ROCK	37.24	-122.13	0.13	-78.6	-20.3	-28.9	1970.5	1974.5
CHA PA	22.35	103.83	0.0	-51.5	-115.3	-175.8	1960.5	1978.5
CHAMBON FORET	48.02	2.26	0.14	-54.3	-24.4	101.6	1960.5	1980.5
CHELYUSKIN II	77.72	104.28	0.0	-32.6	-91.1	-81.0	1960.5	1979.5
COIMBRA	40.22	-8.42	0.09	22.8	-15.1	21.8	1960.5	1980.5
COLLEGE	64.86	-147.84	0.08	-4.2	-52.0	-109.0	1960.5	1982.5
DALLAS	32.99	-96.75	0.20	56.0	17.8	-80.9	1964.5	1974.5
DIKSON II	73.54	80.56	0.01	-87.4	-144.5	-255.6	1960.5	1980.5
DOMBAS II	62.07	9.12	0.65	-68.4	-81.5	-242.4	1960.5	1980.5
DOURBES	50.16	4.99	0.20	20.0	-21.4	78.7	1960.5	1981.5
DRUZHNAYA	80.62	58.05	0.01	72.1	-676.0	1160.5	1960.5	1979.5
DUMONT DURVILLE	-66.66	140.01	0.03	-164.4	-383.0	-2906.7	1960.5	1981.5
DUSHETI	42.09	44.71	0.97	-205.4	-2.6	-102.5	1960.5	1981.5
DYMER	50.72	30.30	0.09	-3.3	81.6	106.0	1964.5	1979.5
EBRO	40.82	0.49	0.04	29.9	-0.1	-25.9	1960.5	1979.5
EIGHTS	-75.23	-77.17	0.44	103.0	203.2	109.7	1963.6	1965.4
ESKDALEMUIR	55.32	-3.20	0.24	18.9	-52.4	-57.9	1960.5	1981.5
FORT CHURCHILL	58.77	-94.10	0.03	-113.2	41.8	-255.2	1964.5	1980.5
FREDERICKSBURG	38.21	-77.37	0.06	84.4	-71.1	135.9	1960.5	1982.5
FUQUENE	5.47	-73.74	2.54	128.5	-76.2	80.0	1960.5	1979.5
FURSTNFELDBRUCK	48.16	11.28	0.56	-5.3	-8.7	5.4	1960.5	1981.5
GNANGARA	-31.78	115.95	0.05	2.9	-126.1	150.8	1960.5	1981.5
GODHAVN	69.24	-53.52	0.0	228.8	-272.6	481.4	1960.5	1975.5
GODHAVN II	69.24	-53.52	0.0	288.7	-310.8	740.2	1976.5	1979.0
GORNOTAYEZHNAYA	43.68	132.17	0.29	4.5	-6.9	-58.6	1960.5	1981.5
GREAT WHALE R	55.27	-77.78	0.02	280.0	107.0	-56.5	1966.5	1980.5
GROCKA	44.63	20.77	0.23	-17.0	-50.0	-60.7	1960.5	1976.5
GUAM	13.58	144.87	0.14	146.8	90.4	94.1	1960.5	1982.5

TABLE 6 (Cont.)

Observatory	Latitude (Deg)	Longitude (Deg)	Altitude (Km)	X Bias (nT)	Y Bias (nT)	Z Bias (nT)	Begin Year	End Year
HALLETT STATION	-72.32	170.22	0.0	110.1	-110.8	-177.9	1960.8	1962.5
HALLEY BAY	-75.52	-26.68	0.02	19.3	380.7	-34.2	1960.5	1975.5
HARTLAND	50.99	-4.48	0.09	-26.9	4.8	52.3	1960.5	1981.5
HATIZYO	33.12	139.80	0.0	-83.4	-1031.7	361.1	1967.7	1982.5
HAVANA	22.97	-82.14	0.0	72.0	162.2	-24.8	1965.5	1978.5
HEL	54.61	18.82	0.0	56.7	-162.0	-89.7	1960.5	1979.5
HERMANUS	-34.43	19.23	0.02	21.4	13.6	20.7	1960.5	1981.5
HOLLANDIA	-2.57	140.51	0.22	-196.3	-61.3	-370.2	1960.5	1962.3
HONGKONG	22.36	114.22	0.02	-66.9	39.0	-33.5	1974.5	1978.5
HONOLULU IV	21.32	-158.00	0.0	-157.5	93.7	-337.5	1961.5	1982.5
HUANCAYO	-12.04	-75.34	3.31	94.9	47.5	15.4	1960.5	1981.5
HURBANOVO	47.87	18.19	0.11	21.6	-19.6	-46.5	1960.5	1979.5
HYDERABAD	17.41	78.55	0.49	330.8	70.1	469.2	1965.5	1980.5
IBADAN	7.43	3.90	0.29	104.1	-325.1	116.7	1960.5	1962.5
ISLA DE PASCUA	-27.17	-109.42	0.0	-15.4	584.9	-498.9	1961.8	1968.4
ISTANBL KNDILLI	41.06	29.06	0.12	202.3	118.6	4.5	1960.5	1979.5
JAIPUR	26.92	75.80	0.0	188.6	-403.8	-32.4	1979.5	1981.5
JULIANEHAAB II	60.72	-46.03	0.45	121.5	-177.3	351.8	1960.6	1964.6
KAKIOKA	36.23	140.19	0.02	5.4	16.3	-80.4	1960.5	1981.5
KANOYA	31.42	130.88	0.10	4.5	62.7	-33.3	1960.5	1981.5
KANOZAN	35.25	139.96	0.34	-38.8	41.8	-54.4	1961.5	1978.5
KELES	41.42	69.21	0.44	-179.8	-53.8	-39.0	1960.5	1963.5
KERGUELEN	-49.35	70.20	0.04	225.7	191.3	661.2	1960.5	1981.5
KIEV	50.72	30.30	0.09	-62.6	188.2	119.2	1960.5	1963.5
KIRUNA	67.83	20.42	0.38	-809.0	-1819.1	-39.5	1965.5	1981.5
KLYUCHI	55.03	82.90	0.0	199.0	-87.5	-18.8	1967.5	1981.5
KODAIKANAL	10.23	77.46	2.32	-528.0	269.9	-47.6	1960.5	1980.5
KOROR	7.34	134.50	0.0	70.8	135.3	151.7	1961.5	1966.2
KRASNAYA PAKHRA	55.48	37.31	0.19	135.9	-18.5	222.3	1960.5	1979.5
KSARA	33.82	35.89	0.91	-23.5	54.7	-87.7	1960.5	1970.5
LA PAZ	-16.54	-68.10	0.42	39.2	97.6	246.6	1974.5	1976.5
LA QUIACA II	-22.10	-65.60	3.44	47.0	-4.3	12.7	1960.5	1982.5
LEIRVOGUR	64.18	-21.70	0.0	-274.5	593.3	-493.3	1960.5	1981.5
LERWICK	60.13	-1.18	0.08	-113.7	166.7	30.1	1960.5	1981.5
LHASA	29.70	91.15	3.65	193.8	29.9	-43.9	1960.5	1974.5
LOGRONO	42.46	-2.50	0.44	21.4	3.5	34.8	1960.5	1976.5
LOPARSKOYE	68.25	33.08	0.19	115.2	333.6	-496.9	1961.5	1980.4
LOVO	59.35	17.83	0.02	60.2	-4.4	-3.3	1960.5	1980.5
LUANDA BELAS	-8.92	13.17	0.05	285.2	-35.0	172.8	1960.5	1982.5
LUNPING	25.00	121.17	0.09	31.4	44.8	51.8	1965.8	1981.5
LVOV	49.90	23.75	0.39	152.2	121.4	144.8	1960.5	1981.5
LWIRO	-2.25	28.80	1.67	263.3	80.8	30.4	1960.5	1970.5
M BOUR	14.39	-16.96	0.0	136.7	17.9	48.9	1960.5	1982.5
MACQUARIE ISLND	-54.50	158.95	0.0	279.5	4.2	305.0	1960.5	1981.5
MAGADAN	60.12	151.02	0.0	-1356.0	352.3	1251.2	1960.5	1966.5
MAJURO	7.08	171.38	0.0	-337.6	50.5	-113.7	1964.8	1966.1
MANHAY	50.30	5.68	0.43	20.4	-13.8	169.3	1960.5	1973.5
MAPUTO	-25.92	32.58	0.04	356.5	35.5	-142.8	1960.5	1982.5
MARION ISLAND	-46.88	37.85	0.0	-849.2	664.1	-1371.5	1973.7	1977.5
MAURITIUS II	-20.09	57.55	0.05	500.5	-221.7	-433.4	1960.5	1965.5
MAWSON	-67.60	62.88	0.0	32.8	21.4	201.4	1960.5	1981.5
MEANOOK	54.62	-113.33	0.67	105.2	6.9	-148.0	1960.5	1980.5
MEMAMBETSU	43.91	144.19	0.03	-224.6	147.4	67.3	1960.5	1981.5
MIRNYY	-66.55	93.02	0.01	-114.5	48.5	-438.7	1960.5	1980.5
MISALLAT	29.51	30.89	0.11	-49.9	67.6	100.4	1960.6	1974.5
MIZUSAWA	39.01	141.08	0.11	-117.2	49.4	-190.9	1969.5	1978.5
MOCA	3.34	8.66	1.34	-68.5	-27.1	349.7	1960.5	1971.5
MOLODEZHNAYA	-67.67	45.85	0.0	-19.6	-101.8	-216.5	1965.5	1979.5
MONTE CAPELLINO	44.55	8.95	0.69	-27.2	-62.5	-569.6	1960.5	1962.5
MOULD BAY	76.20	-119.40	0.14	-19.1	5.4	-41.0	1962.8	1980.5
MUNTINLUPA	14.38	121.01	0.06	-52.7	-51.8	33.3	1960.5	1981.5
NAGYCENK	47.63	16.72	0.15	10.7	-13.8	-54.5	1961.5	1981.5
NAIROBI	-1.33	36.82	1.67	60.8	52.6	-33.3	1964.5	1978.5
NARSSARSSUAQ	61.10	-45.20	0.0	-352.2	265.6	555.9	1968.9	1979.0
NEWPORT	48.26	-117.12	0.77	-28.8	112.8	-127.9	1966.6	1981.5
NIEMEGK	52.07	12.68	0.07	-17.3	-3.8	-82.5	1960.5	1982.5
NOVO KAZALINSK	45.80	62.10	0.0	-90.5	-185.3	-5.1	1974.5	1981.5
NOVOLAZAREVSKAY	-70.77	11.83	0.45	-282.2	62.1	176.2	1961.5	1979.5
NURMIJARVI	60.51	24.65	0.10	299.3	-107.8	94.3	1960.5	1982.5

TABLE 6 (Cont.)

Observatory	Latitude (Deg)	Longitude (Deg)	Altitude (Km)	X Bias (nT)	Y Bias (nT)	Z Bias (nT)	Begin Year	End Year
OTTAWA	45.40	-75.55	0.75	154.1	-148.0	186.1	1968.7	1980.5
PAMATAI	-17.57	-149.57	0.18	-578.7	-1093.3	376.0	1966.2	1972.5
PAMATAI II	-17.57	-149.57	0.08	-642.9	-721.0	-124.0	1973.5	1982.5
PANAGYURISHTE	42.51	24.18	0.55	-172.0	-169.7	-187.9	1960.5	1977.5
PARAMARIBO	5.81	-55.22	0.0	31.0	62.6	-38.2	1960.5	1974.5
PARATUNKA	52.90	158.43	0.10	-329.5	230.1	255.6	1969.5	1979.5
PATRONY	52.17	104.45	0.53	30.9	49.6	-85.4	1960.5	1979.5
PILAR	-31.67	-63.88	0.33	18.6	3.9	-16.4	1960.8	1982.5
PLATEAU	-79.25	40.50	3.61	78.6	-18.1	-27.1	1966.5	1968.5
PLESHENITZI	54.50	27.88	0.19	291.9	155.0	-130.1	1961.5	1981.5
PODKAM TUNGUSKA	61.60	90.00	0.0	66.6	58.5	-307.9	1969.5	1981.5
PORT MORESBY	-9.41	147.15	0.07	25.8	48.7	270.5	1960.5	1981.5
PORT-ALFRED	-46.43	51.87	0.0	-669.9	1218.2	158.8	1974.5	1981.5
PRUHONICE	49.99	14.55	0.32	-24.5	22.7	-82.6	1960.5	1972.5
QUETTA	30.19	66.95	1.74	3.4	49.4	-60.9	1960.5	1981.5
REGENSBERG	47.48	8.44	0.59	26.3	31.8	-35.4	1960.5	1975.5
RESOLUTE BAY	74.70	-94.90	0.02	41.5	29.0	75.6	1960.5	1980.5
ROBURENT	44.30	7.89	0.81	95.2	-18.5	112.9	1964.8	1968.5
ROBURENT II	44.30	7.89	0.81	104.1	56.5	70.5	1969.5	1973.5
ROI BAUDOUIN	-70.43	24.30	0.13	-98.9	-3.3	-24.3	1964.7	1966.5
RUDE SKOV	55.84	12.46	0.04	44.2	-9.7	-46.7	1960.5	1981.5
SABHAWALA	30.36	77.80	0.49	4.4	-54.7	19.5	1964.5	1980.5
SAN FERNANDO	36.46	-6.21	0.02	79.9	39.2	-60.2	1960.5	1978.5
SAN JOSE LAS LA	23.02	-82.65	0.0	64.9	19.9	-10.9	1964.8	1976.2
SAN JUAN	18.38	-66.12	0.09	130.6	43.8	175.5	1960.5	1964.5
SAN JUAN II	18.11	-66.15	0.39	-35.6	197.2	163.4	1965.5	1982.5
SAN MIGUEL III	37.77	-25.65	0.17	719.3	432.4	1713.7	1960.5	1977.5
SANAE	-70.30	-2.37	0.04	-37.4	-31.2	21.2	1962.7	1981.5
SCOTT BASE	-77.85	166.78	0.01	-2260.9	-927.9	-3779.3	1960.8	1979.5
SHESHAN	31.10	121.19	0.09	-220.3	81.4	230.8	1960.5	1980.5
SHILLONG	25.57	91.88	0.0	-108.2	-77.1	-373.9	1979.5	1981.5
SIMOSATO	33.57	135.94	0.05	-41.0	45.9	17.5	1960.5	1977.5
SITKA	57.06	-135.32	0.02	9.5	-9.4	-78.2	1960.5	1981.5
SODANKYLA	67.61	27.05	0.17	-126.7	-117.0	-598.6	1960.5	1982.5
SOUTH GEORGIA	-54.28	-36.48	0.0	-74.6	-359.0	98.1	1975.5	1981.5
SOUTH POLE	-89.99	-13.32	2.79	-1334.5	-3483.0	71.2	1960.5	1971.5
SREDNIKAN IV	62.44	152.31	0.60	110.3	12.1	95.6	1961.5	1966.5
ST JOHN S	47.59	-52.68	0.0	56.3	14.0	1.1	1968.8	1980.5
STEKOLINIY	60.12	151.02	0.0	-266.0	-732.7	49.1	1966.5	1981.5
STEPANOVKA	46.78	30.88	0.13	-101.0	-705.1	62.0	1960.5	1981.5
STONYHURST	53.85	-2.47	0.11	23.7	16.5	-70.4	1961.5	1967.5
SURLARI	44.68	26.25	0.08	28.2	-32.1	-61.6	1960.5	1980.5
SWIDER	52.12	21.25	0.09	-303.6	-105.5	250.3	1960.5	1974.5
SYOWA BASE	-69.01	39.59	0.0	-9.4	-70.8	-17.6	1960.6	1970.5
TAMANRASSET	22.79	5.53	1.37	79.9	-205.6	-10.4	1960.5	1971.0
TANANARIVE	-18.92	47.55	1.37	413.5	5.0	-407.4	1960.5	1981.5
TANGERANG	-6.17	106.63	0.01	-28.7	10.5	-1.1	1964.5	1976.5
TATUOCA	-1.21	-48.51	0.0	51.9	-104.3	160.4	1960.5	1980.5
TEHRAN	35.74	51.38	1.36	-75.8	16.3	-215.1	1960.5	1971.5
TENERIFE	28.48	-16.28	0.30	-444.2	106.2	-1081.8	1960.5	1979.5
TEOLOYUCAN	19.75	-99.18	2.27	-50.0	-9.8	-124.3	1960.5	1975.5
THULE II	77.48	-69.17	0.05	-51.7	97.7	20.9	1960.5	1980.5
TIHANY	46.90	17.89	0.18	2.4	-12.6	-40.6	1960.5	1980.5
TIKSI	71.58	129.00	0.03	-79.1	-151.5	-118.0	1960.5	1979.5
TOLEDO	39.88	-4.05	0.50	15.8	2.6	-4.4	1960.5	1980.5
TOMSK	56.47	84.93	0.19	12.4	-59.1	-242.1	1960.5	1969.5
TOOLANGI	-37.53	145.47	0.45	12.9	-12.6	60.2	1960.5	1979.2
TRELEW	-43.25	-65.31	0.02	121.4	22.2	52.9	1960.5	1978.5
TRIVANDRUM	8.48	76.95	0.29	251.4	182.8	150.6	1960.5	1980.5
TROMSO	69.66	18.95	0.11	98.8	-404.1	171.7	1960.5	1981.5
TSUMEB	-19.22	17.70	0.08	62.9	-80.1	103.8	1964.8	1981.5
TUCSON	32.25	-110.83	0.76	-50.2	-65.5	134.4	1960.5	1981.5
UELEN	66.16	-169.84	0.0	-83.0	33.8	-116.3	1960.5	1979.5
UJJAIN	23.18	75.78	0.0	-232.2	190.0	272.4	1979.5	1981.5
ULAN BATOR	47.85	107.05	0.0	-30.4	-9.5	-118.6	1966.5	1977.5
VALENTIA	51.93	-10.25	0.0	145.4	-56.5	14.6	1960.5	1980.5
VANNOVSKAYA	37.95	58.11	0.56	199.1	97.2	50.5	1960.5	1980.5
VASSOURAS	-22.40	-43.65	0.45	102.4	-67.4	-32.7	1960.5	1981.3

TABLE 6 (Cont.)

Observatory	Latitude (Deg)	Longitude (Deg)	Altitude (Km)	X Bias (nT)	Y Bias (nT)	Z Bias (nT)	Begin Year	End Year
VICTORIA	48.52	-123.42	0.19	28.8	-6.4	-327.7	1960.5	1980.5
VOSTOK	-78.45	106.87	3.49	-5.5	124.7	85.8	1960.5	1979.5
VOYEYKOVO	59.95	30.71	0.06	93.4	17.0	-276.2	1960.5	1981.5
VYSOKAY DUBRAVA	56.73	61.07	0.28	-266.0	-117.3	-512.2	1960.5	1976.5
WHITESHELL	49.75	-95.25	0.0	194.6	-241.7	-237.5	1977.5	1980.4
WIEN KOBENZL	48.26	16.32	0.39	38.0	-2.5	15.3	1960.5	1980.5
WILKES	-66.25	110.58	0.0	656.4	-289.0	19.5	1960.5	1966.5
WINGST	53.74	9.07	0.04	69.5	43.4	-67.7	1960.5	1980.5
WITTEVEEN	52.81	6.67	0.01	35.6	1.8	-81.9	1960.5	1980.5
YAKUTSK	62.02	129.72	0.09	70.3	-1181.3	105.4	1960.5	1979.5
YANGI-BAZAR	41.33	69.62	0.80	-271.2	46.8	-115.0	1964.5	1981.5
YELLOW-KNIFE	62.40	-114.50	0.18	416.6	-212.0	129.6	1975.5	1980.5
YUZHNO SAKH II	46.95	142.72	0.06	51.2	-146.7	-159.6	1960.5	1969.5
YUZHNO SAK III	46.95	142.72	0.06	-73.0	-56.5	99.2	1970.5	1980.5
ZAYMISHCHE	55.83	48.85	0.07	-276.0	-307.6	-258.7	1960.5	1981.5

TABLE 7. STATISTICS OF MODEL DATA SET RESIDUALS RELATIVE TO GSFC (10/84)

	B	X	Y	Z
POGO				
rms	6.8			
mean	-0.3			
sigma	6.7			
MAGSAT				
rms	7.3	6.3	7.9	7.2
mean	-0.1	-0.1	1.3	-3.6
sigma	7.3	6.3	7.8	6.2
Annual Means (with biases)				
rms		15.8	14.8	26.0
mean		-0.1	-0.0	-0.1
sigma		15.8	14.8	26.0
Annual Means (without biases)				
rms		268.5	330.2	457.6
mean		-3.8	-36.7	-30.8
sigma		268.5	328.2	456.5

Figure 1

GSFC 9/84-0 $Z = -B_r$ COMPONENT AT CMB AT 1980

UNITS: GAUSS (10^5 nT)

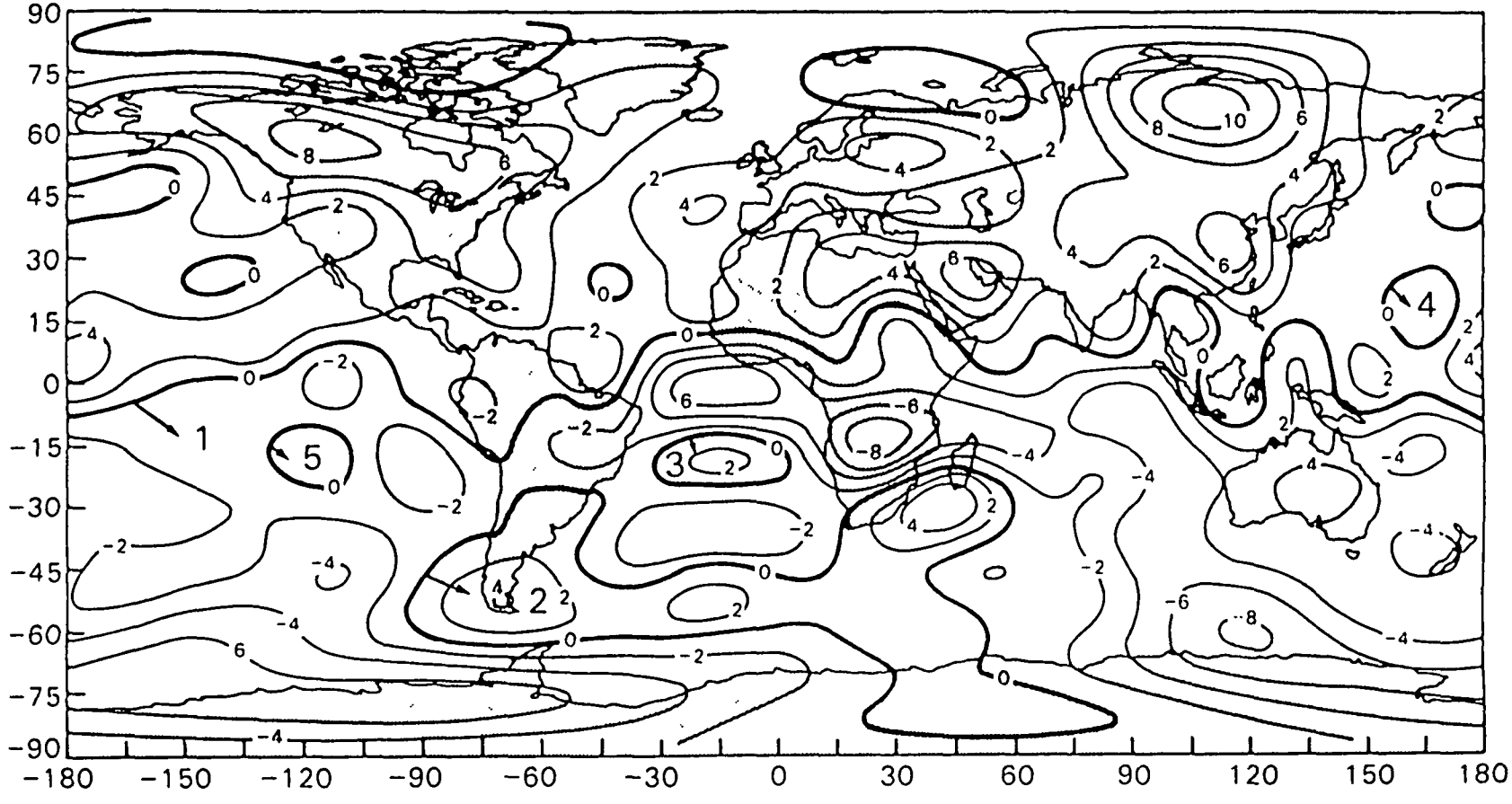

Figure 2

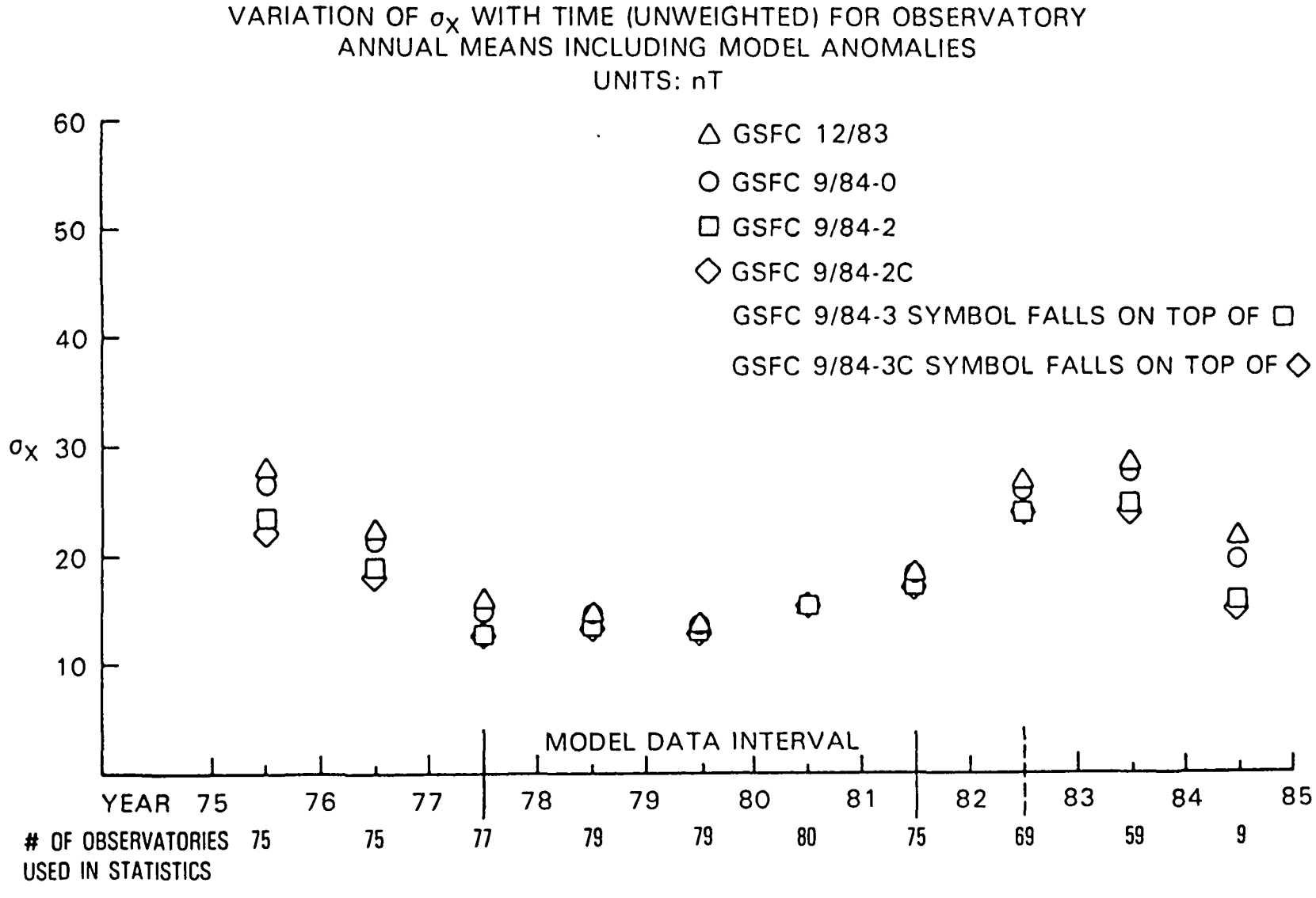
VARIATION OF σ_X WITH TIME (UNWEIGHTED) FOR OBSERVATORY
ANNUAL MEANS INCLUDING MODEL ANOMALIES
UNITS: nT
△ GSFC 12/83
○ GSFC 9/84-0
□ GSFC 9/84-2
◇ GSFC 9/84-2C
GSFC 9/84-3 SYMBOL FALLS ON TOP OF □
GSFC 9/84-3C SYMBOL FALLS ON TOP OF ◇
σ_X
60
50
40
30
20
10
MODEL DATA INTERVAL
YEAR 75 76 77 78 79 80 81 82 83 84 85
OF OBSERVATORIES USED IN STATISTICS 75 75 77 79 79 80 75 69 59 9

Figure 3

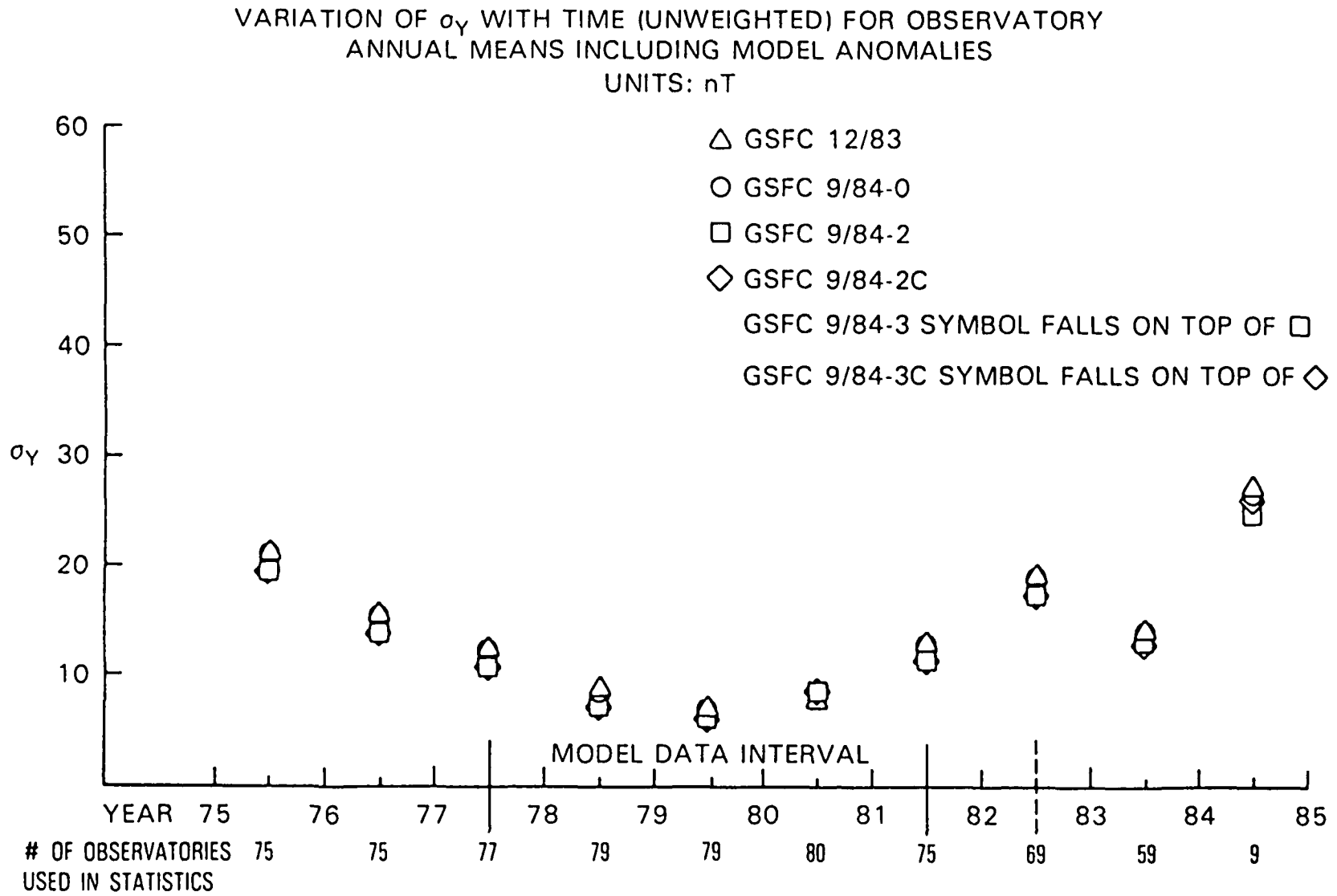
VARIATION OF σ_Y WITH TIME (UNWEIGHTED) FOR OBSERVATORY ANNUAL MEANS INCLUDING MODEL ANOMALIES
UNITS: nT
△ GSFC 12/83
○ GSFC 9/84-0
□ GSFC 9/84-2
◇ GSFC 9/84-2C
GSFC 9/84-3 SYMBOL FALLS ON TOP OF □
GSFC 9/84-3C SYMBOL FALLS ON TOP OF ◇
σ_Y
60
50
40
30
20
10
MODEL DATA INTERVAL
YEAR 75 76 77 78 79 80 81 82 83 84 85
OF OBSERVATORIES USED IN STATISTICS 75 75 77 79 79 80 75 69 59 9

Figure 4

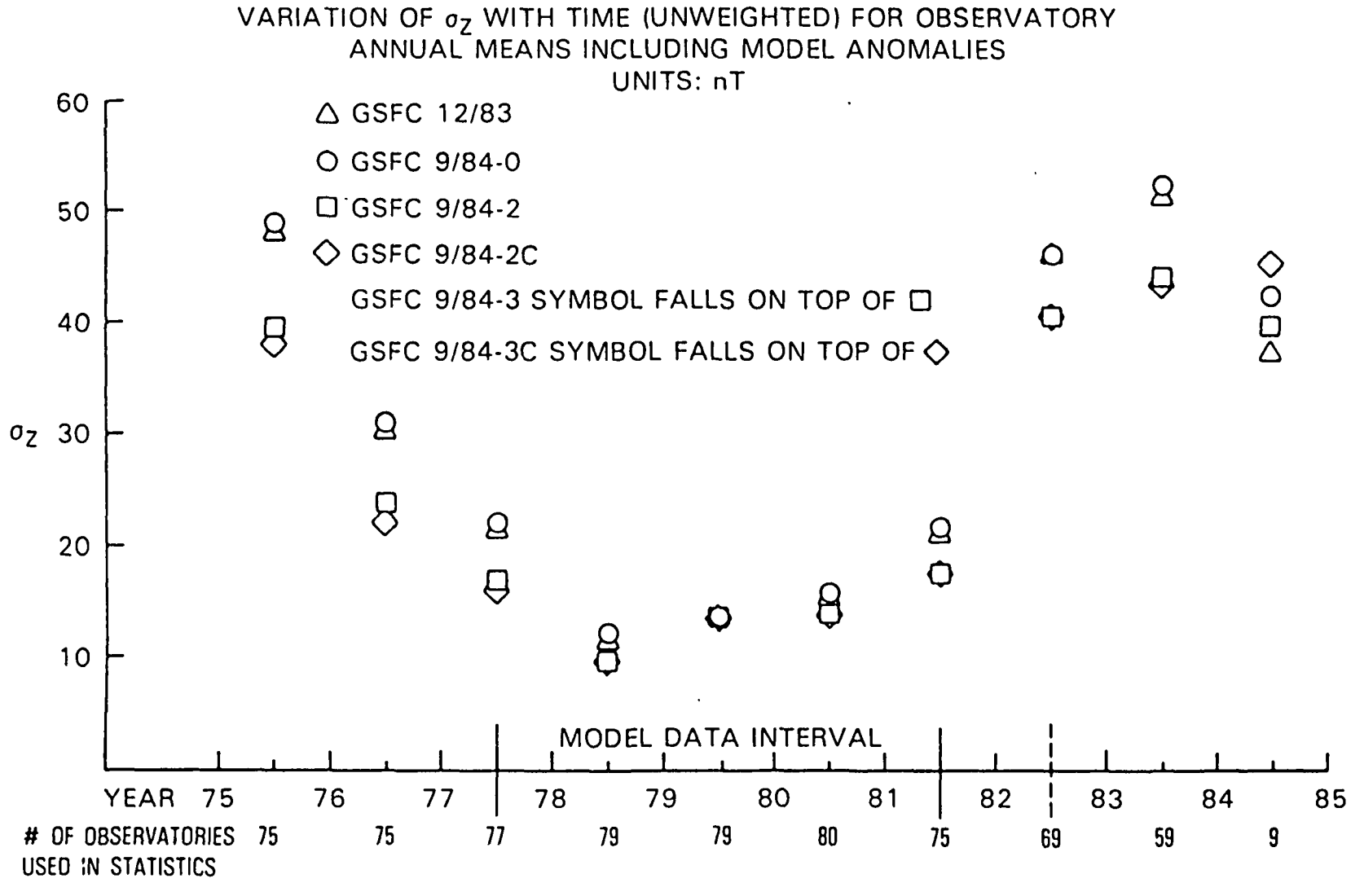
VARIATION OF σ_Z WITH TIME (UNWEIGHTED) FOR OBSERVATORY ANNUAL MEANS INCLUDING MODEL ANOMALIES
UNITS: nT
GSFC 12/83
GSFC 9/84-0
GSFC 9/84-2
GSFC 9/84-2C
GSFC 9/84-3 SYMBOL FALLS ON TOP OF
GSFC 9/84-3C SYMBOL FALLS ON TOP OF
σ_Z
60
50
40
30
20
10
MODEL DATA INTERVAL
YEAR 75 76 77 78 79 80 81 82 83 84 85
OF OBSERVATORIES USED IN STATISTICS 75 75 77 79 79 80 75 69 59 9

Figure 5

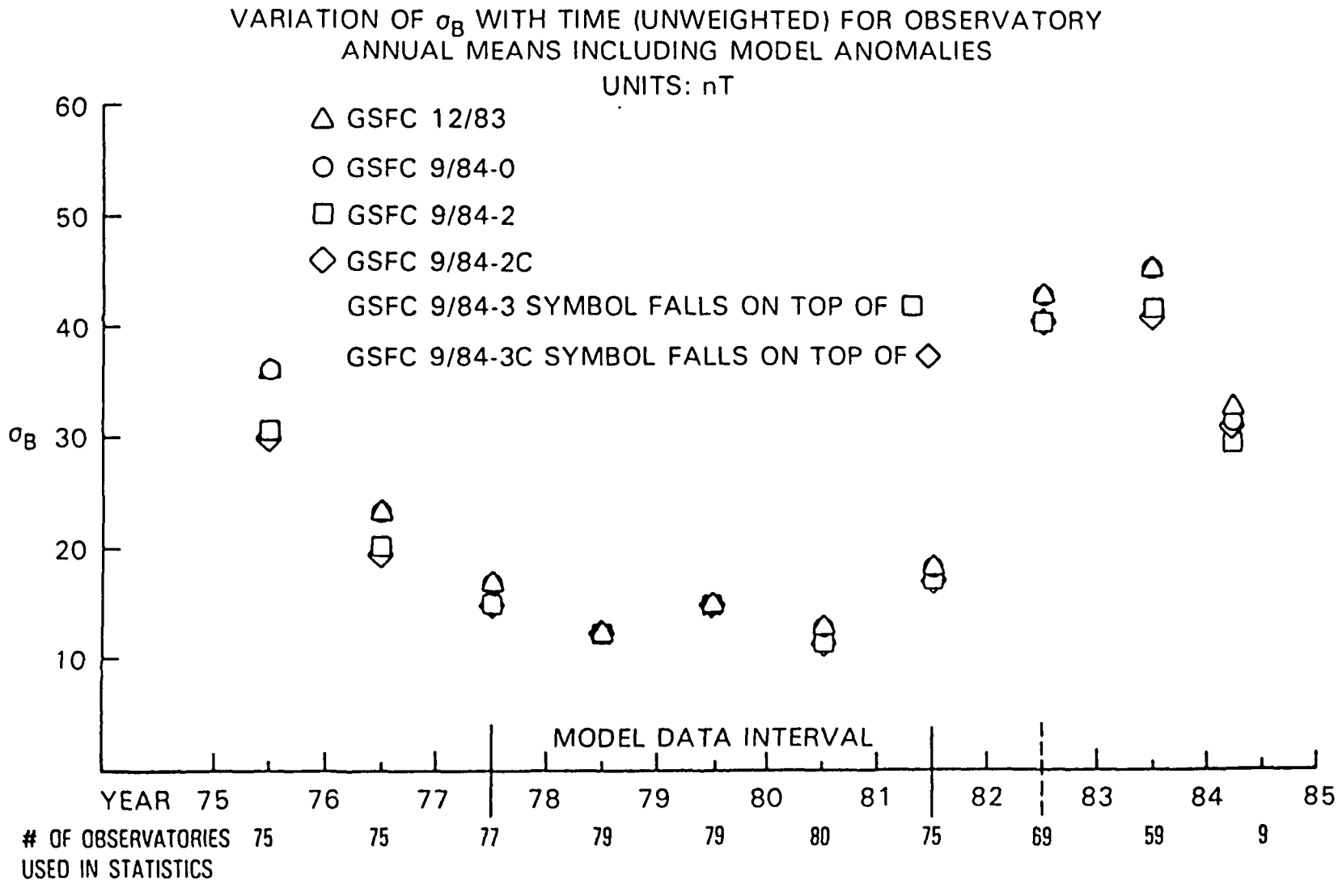
VARIATION OF σ_B WITH TIME (UNWEIGHTED) FOR OBSERVATORY ANNUAL MEANS INCLUDING MODEL ANOMALIES
UNITS: nT
△ GSFC 12/83
○ GSFC 9/84-0
□ GSFC 9/84-2
◇ GSFC 9/84-2C
GSFC 9/84-3 SYMBOL FALLS ON TOP OF □
GSFC 9/84-3C SYMBOL FALLS ON TOP OF ◇
σ_B
60
50
40
30
20
10
MODEL DATA INTERVAL
YEAR 75 76 77 78 79 80 81 82 83 84 85
OF OBSERVATORIES USED IN STATISTICS 75 75 77 79 79 80 75 69 59 9

Figure 6

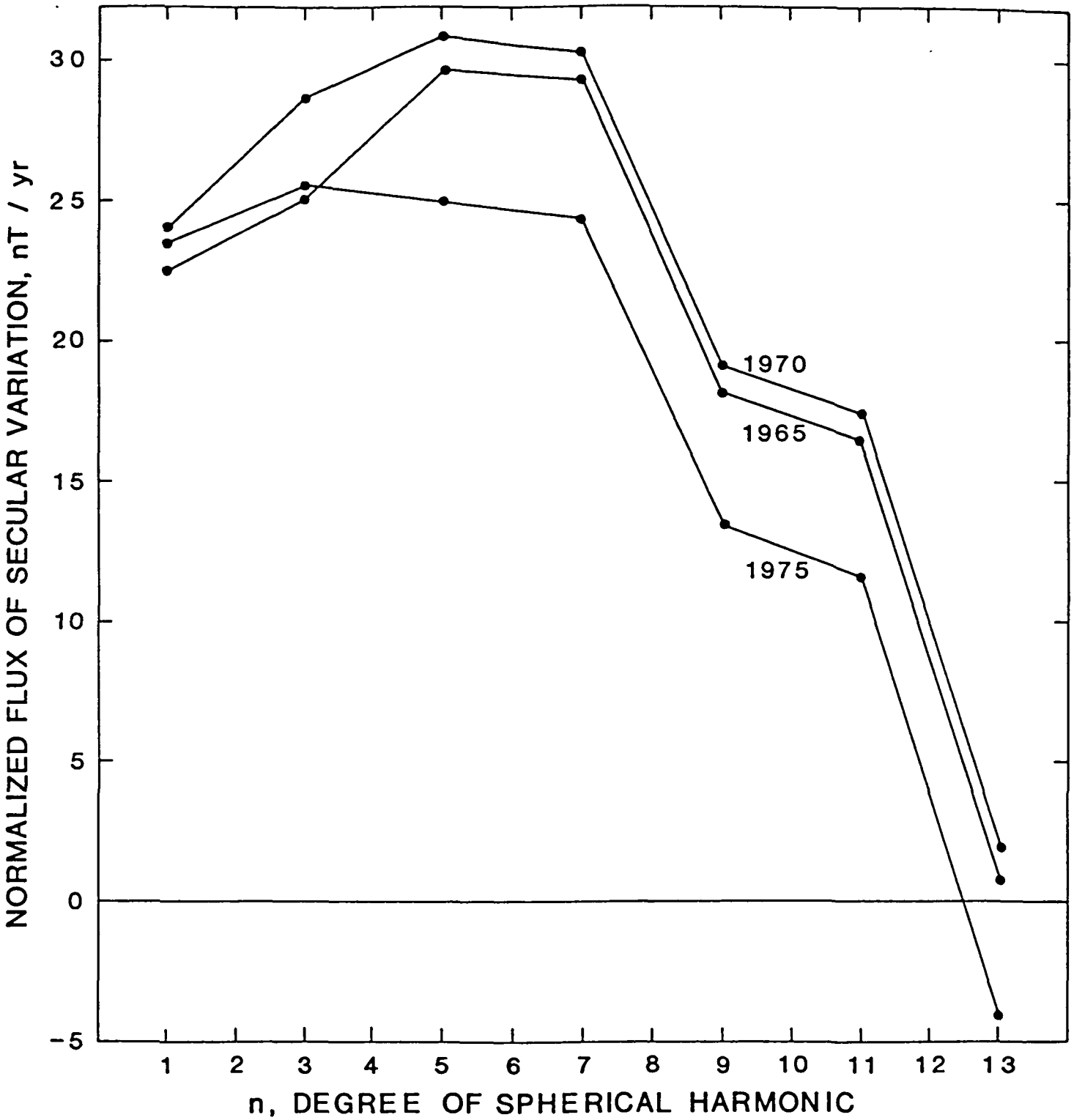

Normalized Flux of Secular Variation Through the Northern Geographic Hemisphere of the Core-Mantle Boundary

$$\left(\frac{1}{2\pi (a/b)^3} \int_0^{2\pi} \int_0^{\pi/2} \frac{\delta Br}{\delta t} \sin\theta d\theta d\phi, \text{ in } nT/yr \right)$$

as a Function of Spherical Harmonic Degree According to GSFC 10/84.

Appendix A. Derivation of an Analytic, Linear Constraint on Secular Variation

In the absence of cross-equatorial flow implied by (9), the geographic equator on the CMB always consists of the same fluid parcels (Benton, 1985, Backus and LeMouel, 1986). Hence, (6) shows that the total (not absolute) magnetic flux, M_0, out of, say, the northern geographic hemisphere of the CMB is conserved:

$$M_0 = \int_0^{2\pi} \int_0^{\pi/2} B_r(b,\theta,\phi,t) b^2 \sin\theta d\theta d\phi = \text{constant} \quad . \tag{A1}$$

If the mantle is an insulator then (c.f. Chapman & Bartels, 1940)

$$B_r(b,\theta,\phi,t) = \sum_{n=1}^{N} \sum_{m=0}^{n} (n+1) \left(\frac{a}{b}\right)^{n+2} \cdot$$

$$\left[g_n^m(t) \cos m\phi + h_n^m(t) \sin m\phi\right] P_n^m(\theta) \tag{A2}$$

where a = 6371.2 is the earth's radius, g_n^m, h_n^m are the time-dependent Gauss coefficients of order m, degree n, $P_n^m(\theta)$ is the Schmidt quasi-normalized associated Legendre function and N is the degree of truncation. Insertion of (A2) into (A1) followed by integration with respect to ϕ leads to

$$M_o = 2\pi b^2 \sum_{n=1}^{N} (n+1) \left(\frac{a}{b}\right)^{n+2} g_n^o \int_o^1 P_n^o(\mu)d\mu, \ \mu = \cos\theta \ . \qquad (A3)$$

The integral can be carried out readily in terms of the differential definition of P_n^o (Chapman & Bartels, 1940):

$$P_n^o(\mu) = \frac{1}{2^n(n!)} \frac{d^n}{d\mu^n}[(\mu^2-1)^n] \qquad (A4)$$

Thus,

$$\int_o^1 P_n^o(\mu)d\mu = \frac{1}{2^n(n!)} \left\{\frac{d^{n-1}}{d\mu^{n-1}}[(\mu^2-1)^n]\right\}_{\mu=0}^{\mu=1} . \qquad (A5)$$

The quantity in curly brackets here can be identified with the coefficients of degree $n-1$ in Taylor series expansions of the function

$$f(\mu) = (\mu^2-1)^n \ . \qquad (A6)$$

First expand $f(\mu)$ in powers of μ^2-1, and then expand in powers of μ. In this way one finds that

$$\left\{\frac{d^{n-1}}{d\mu^{n-1}}[(\mu^2-1)^n]\right\}_{\mu=1} = 0 \ .$$

$$\left\{\frac{d^{n-1}}{d\mu^{n-1}}[(\mu^2-1)^n]\right\}_{\mu=0} = (-1)^{(n+1)/2} \frac{(n!)(n-1)!}{[(\frac{n+1}{2})!][(\frac{n-1}{2})!]} \ , \text{for n odd}$$

$$= 0 \ . \qquad , \text{for n even} \qquad (A7)$$

Accordingly, (A3) can be written as

$$M_o = 2\pi b^2 \sum_{n=1,3,5,\ldots} \frac{(-1)^{\frac{n-1}{2}}}{2^n n} \frac{(n+1)!}{\left[\left(\frac{n+1}{2}\right)!\right]\left[\left(\frac{n-1}{2}\right)!\right]} \left(\frac{a}{b}\right)^{n+2} g_n^o = \text{constant} \qquad (A8)$$

Division by $2\pi(a^3/b)$ followed by time differentiation then leads to the expression in (11) of the text, when the multiplicative constants are expressed recursively.

Appendix B. A New Unconstrained Field Model, GSFC(10/84)

The GSFC(10/84) geomagnetic field model is a spherical harmonic representation of the earth's field based on data spanning the years 1960 through 1982. It is essentially a remake of GSFC(9/80), Langel et al. 1982, using an improved MAGSAT data set, additional observatory data and a time-dependent representation for external field effects. The earth's field is assumed to be derivable from the gradient of a magnetic scalar potential

$$V(r,\theta,\phi,t) = a \sum_{n=1}^{N_1} \sum_{m=0}^{n} \left(\frac{a}{r}\right)^{n+1} [g_n^m(t)\cos m\phi + h_n^m(t)\sin m\phi] \cdot P_n^m(\theta)$$

$$+ a \sum_{n=1}^{N_2} \sum_{m=0}^{n} \left(\frac{r}{a}\right)^{n} [q_n^m(t)(\cos m\phi + s_n^m(t)\sin m\phi]P_n^m(\theta) \qquad . \quad (B1)$$

where N_1, N_2 are truncation levels for the expansions of the internal and external fields. The Schmidt normalized internal Gauss coefficients, g_n^m, h_n^m, for GSFC(10/84) are presented in Table 4 at epoch 1980 to order and degree N_1 = 13 for the main field and its first time derivative, with N_1 = 6 and 4, respectively, for the second and third time derivatives. In contrast to GSFC(9/80) but in common with the GSFC(12/83) model, Langel and Estes (1985), the first degree external terms and corresponding induced internal terms are modeled as linear functions of Dst, while fixed biases, or anomalies, are estimated for each observatory in the solution, as described by Langel et al.

(1982).

The observations selected for this model are comprised of POGO and MAGSAT data plus observatory annual means. The POGO data consist of 35,780 scalar measurements obtained by selecting every other observation from the time-ordered POGO data set used for GSFC(9/80). These data span the interval from December 1964 through June 1971. The MAGSAT data consist of the 54,813 corrected, quiet day vector and scalar measurements used in deriving the GSFC(12/83) model. The annual means data set spanned the years from 1960.5 to 1982.5 for a total of 3196 vector measurements (9588 total observations from 206 observatories selected out of the NOAA National Geophysical and Solar Terrestrial Data Center, Release 31 data set). Table 5 lists the number of observatories used in the solution by year, while Table 6 names and locates each observatory together with its anomaly bias from the solution and its overall data interval used. Stations whose records were not continuous in time were given unique names for each interval of continuity (e.g. Baker Lake, Baker Lake II, Baker Lake III, etc) and each was treated as an independent observatory in the solution. Observatory data were converted from any three independent scalars (i.e. D,H,B etc) to X,Y,Z components in a geodetic coordinate system assuming an equatorial radius of 6398.165 km and a reciprocal flattening of 298.25. Annual averages of Dst were used in processing annual means data.

The external field coefficients for GSFC(10/84) are

$$q_1^0 = 18.48 - 0.64\,\mathrm{Dst\ (nT)} \qquad \text{(B2)}$$

$$q_1^1 = -1.25 + 0.02\,\mathrm{Dst\ (nT)} \qquad \text{(B3)}$$

$$s_1^1 = -3.31 + 0.15\,\mathrm{Dst\ (nT)} \qquad \text{(B4)}$$

The corresponding g_1^0 internal coefficient, including the effects of currents induced by the time-varying external field, is

$$g_1^0 = -29{,}992.1 + 0.33\,q_1^0\ \mathrm{(nT)} \quad . \qquad \text{(B5)}$$

Induced contributions to g_1^1, h_1^1, considered negligible, were not computed. Table 7 gives the unweighted statistics of the misfit between the satellite and observatory data used in the model and the model itself. For the observatories, the statistics are presented both with and without the biases.